CO_2-EOR: Security of Storage

31 March 2015

Peter Olden, Heriot Watt University
Eric Mackay, Heriot Watt University
Gillian Pickup, Heriot Watt University
Jamie Stewart, University of Edinburgh
Gareth Johnson, University of Edinburgh

Scottish Carbon Capture & Storage

Murchison House, West Mains Road Edinburgh EH9 3LA
Telephone +44 (0)131 650 0270 www.sccs.org.uk

Executive Summary

Preliminary studies from CO_2-EOR in Canada have suggested that, in CO_2-EOR settings, solubility trapping takes place within both aqueous and hydrocarbon phases. As such it is postulated that CO_2-EOR may provide a greater quantity of securely stored CO_2 than a purely non-EOR storage operation.

This study's principal objective was to quantify how much solubility trapping takes place within both aqueous and hydrocarbon phases in CO_2-EOR settings.

The Pembina Cardium CO_2 Monitoring Pilot Project was used as a test site to determine the relative roles of solubility trapping. Firstly two geochemical approaches using empirical data from the site (gas geochemistry, production volumes and water isotope geochemistry) were used to determine the phase distribution of CO_2 (dissolved or free phase) at a number of production wells that were sampled monthly during a two-year CO_2 injection pilot. In addition a simplified reservoir simulation was performed to use it as a test-bed to investigate various CO_2 injection scenarios with a model having some of the salient features of the pilot project. In particular this model was used to test the observations of the role of solubility trapping versus free-phase CO_2 trapping.

The two geochemical methods show that the distribution of CO_2 in the reservoir, and hence the relative role of the trapping mechanisms, is closely matched where conditions permit both methods to work. The initial reservoir model simulation also closely matches the average CO_2 distribution and relative trapping contributions derived from the geochemical approaches giving extra confidence in both the methods using the empirical data and the reservoir model itself. After just 2 years of injection it is shown that up to 25-32% of the injected CO_2 is solubility trapped.

Subsequently the reservoir model was used to model a number of alternative scenarios including; continuous CO_2 injection, WAG, injection into a depleted oil field and a saline aquifer. Results show that additional CO_2 storage by solubility trapping is achieved when an oil phase is present (25-50% solubility trapping after 5 years of injection and 45 years of equilibration) relative to a saline aquifer (<25% solubility trapping after 5 years of injection and 45 years of equilibration) hence increasing CO_2 security by reducing the proportion of injected CO_2 that remains as a buoyant free phase.

Contents

1. Introduction

The fate of CO_2 is an important consideration when injecting CO_2 into the geological subsurface. CO_2 can be trapped structurally and stratigraphically, by residual trapping, solubility trapping, and by mineral trapping (IPCC 2005). Although in a well selected storage complex a combination of each of these trapping mechanisms should lead to extremely high confidence in storage security, certain geological risks will always exist (Worden & Smith 2004). What is known however is that the highest geological storage risks exist when CO_2 is in free phase and is reliant of structural and stratigraphic trapping. Increased security of CO_2 storage will be achieved if the storage mechanism migrates from structural and stratigraphic trapping to solubility trapping in the time frame of operations (Figure 1). Therefore to quantify storage security it is important to predict the fate of in-situ CO_2 by understanding the likely contributions of each trapping mechanism in different geological storage circumstances. One of these geological circumstances where CO_2 trapping mechanisms are often not considered is CO_2-EOR, which may be used as a permanent geological store for captured anthropogenic CO_2. This study addresses the issue of storage security in CO_2-EOR settings with particular attention being paid to solubility trapping.

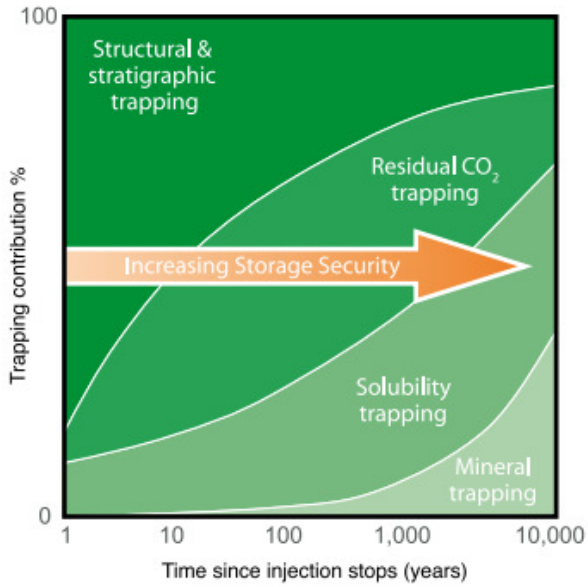

Figure 1: CO_2 storage security over time and trapping mechanisms. (IPCC, 2005)

1.1 Objective and Report Structure

Preliminary studies from CO_2-EOR in Canada (Johnson, 2010) have suggested that, in CO_2-EOR settings, solubility trapping takes place within both aqueous and hydrocarbon phases. As such it is postulated that CO_2-EOR may provide a greater quantity of securely stored CO_2 than a purely non-EOR storage operation.

This study's principal objective was to quantify how much solubility trapping takes place within both aqueous and hydrocarbon phases in CO_2-EOR settings.

Section 1 of this report provides an introduction to the principal trapping mechanisms and to CO_2 solubility in the different phases investigated. Section 2 provides an introduction to the case study used in the following sections, the Pembina Cardium CO_2 Monitoring Pilot Project (PCCMPP). The main technical work of this study was undertaken in three parts as outlined in the following sections of this report:

Section 3 – Use of a geochemical model combined with production data to quantify CO_2 dissolution into oil and brine phase for the PCCMPP and ultimately quantifying the extent of structural, stratigraphic and residual trapping versus solubility trapping during the 2 year CO_2 injection period. In parallel, pore-space saturations were calculated from empirical data using the oxygen isotope approach developed by Johnson (2010). The field chosen has 2 injection wells and 8 production wells over two five-spot patterns. The results from monthly sampling events over a two year injection period of the two methods are compared and phase saturations at discrete time intervals discussed.

Section 4.1 – A simplified reservoir model was constructed to represent the PCCMPP. Using the injection and production data from the field an initial simulation was run to represent the 50 year water flooding history of the reservoir followed by 2 years of CO_2 injection and followed by equilibration over 500 years. The post injection results are compared to the results from section 3. This provides a calibrated attempt at quantifying trapping mechanisms for a two year CO_2 injection period in a CO_2-EOR pilot.

Section 4.2 – The model developed in section 4.1 was then run for alternative scenarios:

1. Continuous CO_2 injection for 5 years post 50 years water flood.
2. Water alternating gas (WAG) injection on a 3 month cycle for 5 years post 50 years of water flood.

3. As a depleted oil field for 5 years post 50 years water flood.
4. As an aquifer with continuous CO_2 injection for 5 years.

This provides quantification of the relative amount of CO_2 securely stored by solubility trapping in each scenario.

Section 5 of this report summarises the conclusions of the study and provides recommendations for further work.

1.2 Trapping Mechanisms

The trapping of CO_2 within a CO_2 injection (storage or EOR) project can be achieved in a number of ways. These include: stratigraphic and structural trapping; residual (hydrodynamic) trapping; solubility (ionic) trapping, and; mineral trapping (IPCC, 2005) (Fig. 1).

Structural and stratigraphic trapping refer to the trapping mechanisms where CO_2 accumulates as a free phase within a reservoir rock. These traps require some form of physical closure, for example, an impermeable unit such as a shale as a caprock with an anticline as an accumulation area, or a fault seal or a stratigraphic trap. These traps are most often observed in hydrocarbon exploration. Structural and stratigraphic trapping is considered the least secure of the trapping mechanisms (Fig. 1) as the buoyant free phase CO_2 has a natural tendency to migrate towards the surface. Residual trapping occurs on a longer timescale where the CO_2 is trapped in the interstitial pores of the reservoir rock as the injected CO_2 plume migrates throughout the subsurface. The plume will typically migrate up-dip due to buoyancy until CO_2 dissolution occurs and the CO_2 migrates along with the regional fluid flow (IPCC, 2005). Knowledge of the hydrodynamic flow paths and direction are critical to this form of trapping where no geological closure is necessarily required. Although the CO_2 remains as a free phase it becomes isolated and unconnected in the pores as the CO_2 drains and water re-enters (imbibition) the pore-space and thus the capillary forces are high enough that the CO_2 cannot migrate. Solubility trapping is the dissolution of CO_2 into any reservoir fluid present. This form of trapping again increases the security of storage as explained above (dissolved CO_2 is less buoyant than free phase CO_2). It increases with time as more reservoir fluids are contacted and can be enhanced by CO_2-water-rock reactions that allow more CO_2 dissolution. Mineral trapping, considered the most secure form of trapping is the conversion of CO_2 to a solid mineral precipitate. The geochemical reactions that take place are believed to be slow (1000s of years) and thus the timescales involved are much greater than those for the other trapping mechanisms but in some cases may provide significant trapping in the long term.

In this study we compare the relative amounts of free-phase and solubility trapping. That is we do not separate structural and stratigraphic trapping from residual trapping as both are free phase (non-dissolved) CO_2. Conversely for solubility trapping we

further divide this into two subdivisions; aqueous phase and hydrocarbon phase trapping.

1.3 CO_2 Solubility

CO_2 solubility in Oil

A number of studies have used an experimental approach to determine the solubility, swelling factors and viscosity changes, of CO_2 and crude oil. Welker & Dunlop (1963) experimentally determined these properties in 5 different crude oils ranging from 17-40.2 API over a temperature range of 27.7^{0}C -71.1^{0}C and at pressures up to 5.5MPa. Simon & Graue (1965) published data on these factors for nine different oils (11.9-33.3 API) over a range of temperatures (38-121^{0}C) and up to pressures of 15.9 MPa. The results from their widely used experimental solubility values are shown in Figure 2. Using their experimental results Simon & Graue (1965) also presented correlations for predicting solubility, swelling and viscosity behaviour of CO_2 in oil systems. As described in Chung et al. (1988) these correlations were the principal correlations used in reservoir simulators at the time. Chung et al. (1988) note however that their methods are based on mole fractions rather than mole volumes as their compositional units. This means that the molecular weight of the oil must be known from experimental determination. Using a similar method to Miller & Jones (1981), Chung et al. (1988) experimentally assessed the behaviour of viscosity, swelling factor and solubility of CO_2 over a range of temperatures and pressures (24,60 & 94^{0}C and 1.4-34.5 MPa) for five different heavy oils. These results used a compositional unit of 'volume fraction' giving solubility results in scf/bbl. More recently DeRuiter et al. (1994) used similar experimental procedures to assess the solubility and displacement behaviour of a viscous crude with both CO_2 and a number of hydrocarbon gases.

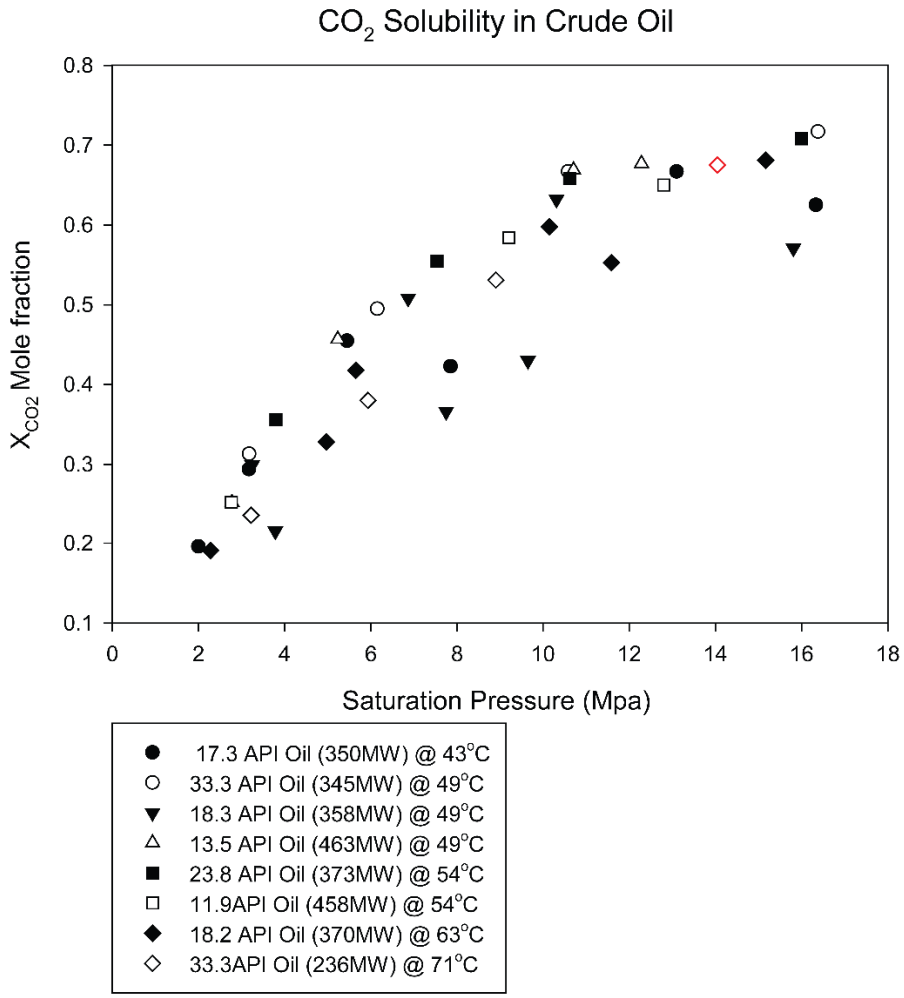

Figure 2 – Experimentally derived CO_2 solubilities in crudes of varying API, Molecular Weight and at different temperatures. Data taken from Simon & Graue (1965)*. The data point in red portrays the experimental conditions closest to those at the Pembina Cardium CO_2EOR Pilot.*

Although testing different oils with a range of experimental procedures, the studies mentioned above have come to similar conclusions. The solubility of CO_2 in oil is controlled predominantly by reservoir pressure, temperature and to a smaller extent the oil API gravity (Simon & Graue 1965; Welker & Dunlop 1963; Chung et al. 1988; DeRuiter et al. 1994). Generally solubility increases with pressure and oil API gravity (i.e higher in lighter oils) but decreases with temperature. The solubility of CO_2 in oil however does not increase linearly. Figure 2 shows that at lower temperatures and at pressures above 1000 psi (6.9 MPa) the CO_2 solubility is not strongly controlled by pressure (Chung et al. 1988). This phenomenon was also found by DeRuiter et al. (1994) who found that at a temperature of 18.3^{0}C the solubility of CO_2 in the two oils tested increased with pressure until the liquefaction pressure of CO_2 is reached

(5.5Mpa) after which the solubility remains almost constant.

CO_2 Solubility in Water

A number of studies have used an experimental approach to look at the effect of solubility in CO_2-H_2O mixtures. As highlighted by Spycher et al. (2003) initial work focussed on the study of metamorphic processes with high temperatures and pressures (several hundred degrees and up to several kilobar). However more recently studies have used pressure and temperature ranges that are more aligned with hydrocarbon basins. A number of studies such as Diamond & Akinfiev (2003), Spycher et al. (2003) and Duan & Sun (2003) have extensively reviewed experimental work on solubility in CO_2-H_2O systems. Duan & Sun (2003), show that experimental conditions have varied over a range of 1- 3500 bar (0.1-350 Mpa) and 273- 800K (0-527°C) and with different solution properties ranging from pure water to solutions with 4-6 m NaCl.

The results of solubility experiments have been used by a number of studies such as Crovetto (1991) and Carroll & Mather (1992) to derive Henrys law constants for CO_2 in water. Spycher et al. (2003) who developed a new calculation method using Redlich-Kwong equations of state (EOS) for CO_2 and H_2O, to develop aqueous solubility constants, found that the results of their new approach closely matched the constants found by Crovetto (1991) and Carroll & Mather (1992). Solubility results from experimental studies discussed in Spycher et al. (2003) are summarised in an appendix in Spycher et al. (2003). Solubility's of CO_2 in water displayed range from 2.77 mole % CO_2 at 12°C and 34.5 bar (3.45Mpa) to 3.15 mole % CO_2 at 110°C and 700 bar (70Mpa).

The solubility of CO_2 in aqueous fluids in primarily dependant on temperature, pressure and much like the solubility of CO_2 in oil the solubility of CO_2 in brine decreases with temperature but increases rapidly with increasing pressures up to the saturation pressure (Spycher et al. 2003). As noted by Spycher et al. (2003) the solubility trend is also affected by the critical temperature. Below the critical temperature the CO_2 solubility trend shows two distinct phases accounting for liquid CO_2 above saturation pressures and gaseous CO_2 below these pressures. This results in two solubility curves below the critical temperature and one CO_2 solubility trend above the critical temperature.

Alongside Spycher et al. (2003) a number of studies such as Bamberger et al. (2000), Shyu et al. (1997), Duan et al. (1992) and Duan & Sun (2003) have developed

correlations to compute mutual solubility's of CO_2 and H_2O, and more specifically the solubility of CO_2 in H_2O (Carroll & Mather 1992; Crovetto 1991). Of these studies one of the most commonly used correlations is the Duan & Sun (2003) correlations which are also available through their web based calculator. In this work the chemical potential of CO_2 in the vapour phase is calculated using the equation of state (Duan et al. 1992) and the chemical potential of CO_2 in the liquid phase is described by the specific interaction model of Pitzer (1973). The thermodynamic correlations developed by Duan & Sun (2003) can be applied over 272 to 533K (0-260°C) at pressures of 0-2000bar (0.1-200 Mpa) and with waters of 0 to 4.3 M ionic strength (salinity). Duan & Sun (2003) state that model predictions can be matched to experimental data to within 7% in CO_2 solubility, which equates to experimental uncertainty.

2. The Pembina Cardium CO_2 Monitoring Pilot Project (PCCMPP)

The Pembina Cardium CO2 Monitoring Pilot site is located near the town of Drayton Valley, west of Edmonton, (Fig. 3) in the Pembina Field. The Pembina oilfield is the largest individual (Owen, 1975) and one of the oldest onshore oilfields in Canada. The Cardium Formation is a siliciclastic reservoir at approximately 1650 m depth and reservoir temperature and pressure of 50°C and 19MPa respectively (Hitchon, 2009).

Over 11,700 wells have been drilled into the Pembina Field since its discovery in 1953 with oil and gas production from shallow Cretaceous reservoirs of the Paskapoo and Scollard formations to the Upper Devonian carbonate reefs of the Nisku Formation (Dashtgard et al., 2008). The most prolific oil-producing horizon is the Cardium Formation which was discovered in 1953 with the Socony Seaboard Pembina No.1 well located at 04-16-048-08W5 (Dashtgard et al., 2008). Original oil-in-place (OOIP) is estimated to have been 1,180 x 106 m^3 which represents 18.4% of all oil pools in Alberta, Saskatchewan and Northeastern British Columbia (Krause et al., 1987). By 1958 oil production was approximately 16,000 m^3 per day from over 2300 wells that was only restricted by the demand at the time, with a cumulative total of over 16 million m^3 of oil equating to one fifth of total Canadian production and one eighth of total Canadian demand for oil (Stevens et al., 1959). Water-flood pilots were initiated by Pan American Petroleum in 1956 in an effort to counter both production declines and increasing gas:oil ratios (Stevens et al., 1959). They proved successful and by 1958 had reached 10,000 m^3 day of water injection sourced from the North Saskatchewan River (which runs along the southern and eastern portion of the field) and from shallow aquifers (Justen, 1957, Justen and Hoenmans, 1958, Stevens et al., 1959). Water injection volumes rose to a peak of 55,000 m^3 a day by 1973 as oil production peaked in 1970-1972 (Krause et al., 1987) at approximately 20,000 m^3 of oil a day. By 2004 total production from the Cardium Formation by primary and secondary recovery schemes was near the maximum recoverable for the pool, hence tertiary recovery by CO2-EOR was being evaluated and begun in 2005 (Dashtgard et al., 2008).

Geology of the Pembina Field

The Conacian-Turonian (88.5 Ma) Cardium Formation is located near the middle of the 650 m thick Colorado Group Shale (Dashtgard et al., 2008), overlain by the First

White Speckled Shale and underlain by the Blackstone Formation Shale. It is a clastic wedge that prograded into the Western Interior Seaway at the time of deposition (Krause et al., 1994, Plint et al., 1986). The Cardium Formation is sub-divided into 4 reservoir units separated by either shale or sandy-shale beds: the lower sandstone, middle sandstone, upper sandstone and conglomerate. The three sandstone units are compositionally similar and are classified as sub-mature to mature lithic to quartz arenites while the conglomeratic unit varies from clast-supported, quartzose conglomerate to matrix-supported quartzose diamictite (Dashtgard et al., 2008).

Structurally the regional dip in the area is to the southwest. Net pay of the four reservoir units in the Cardium Formation vary from 0-6 metres with the middle sandstone being the thickest in the vicinity of the CO2 injection wells. Typical thickness of the whole reservoir is on the order of 15-20m. Regional stress regime studies indicate the largest principal stress is vertical and the minimum horizontal stress is orientated between 120° and 149° (Bell and Bachu, 2003). If fractures occur they will open in a plane perpendicular to the minimum stress, thus at the Pembina Pilot, fractures will occur vertically with a strike between 30° to 59°, i.e. in a NW-SE direction (Hitchon,2009).

The reservoir is non-uniformly stratified with generally low permeabilities (conglomerate, 160 md, upper sandstones, 17 md, lower sandstones, 2 md) (Krause et al., 1987). Porosity varies from an average of 7.4% in the conglomerate, to 16.4% in the upper sandstone, 16.2% in the middle sandstones and 14.8% in the lower sandstone (Dashtgard et al., 2008).

Geological interpretation of the formation has suggested various potential depositional settings ranging from turbiditic to offshore bars, deltaic and beach and shoreface (Hitchon, 2009 and references therein). At present it is considered that the Cardium Formation sands prograded to the northeast as a series of parasequences followed by subaerial erosion (Krause and Nelson, 1984, Plint et al., 1988, Leggitt et al., 1990). The southwestward transgression over the erosional surface is marked by conglomerate deposition with gravels delivered to the shoreline by fluvial systems and subsequent reworking by shoreline waves (Bergman and Walker, 1987, Arnott, 1992).

CO_2 EOR Pilot at the Pembina Field

The CO_2-EOR pilot was undertaken to examine the possibility of stimulating oil production using a CO_2 flood under the Royal Credit Programme of the Alberta Department of Energy in 2003 (Shevalier et al. 2009). The CO_2-EOR Monitoring Pilot Project was also developed to test the CO_2 storage potential of the Cardium Formation. The pilot consists of two five-spot injection patterns, with two of the production wells being shared by the two injector wells. This results in 2 CO_2 injectors with six surrounding producers (See Figure 3 and 11). These wells occur in the middle of the Pembina field in an area that has been water flooded since 1962 (Dashtgard et al. 2008).

CO_2 injection started in 2005 with approximately 75,000 tons of truck delivered liquid CO_2 being injected between March 2005 and March 2008. Between March 2005 and March 2007 CO_2 was continuously injected through the two injection wells. After this period the pilot switched to WAG injection with injected CO_2 being periodically alternated with water injection. Prior to CO_2 injection baseline reservoir fluid and gas samples were taken to allow for baseline geochemical analysis. Following the initiation of CO_2 injection in March 2005, reservoir fluid and gas samples were taken from each production well at roughly monthly intervals giving 28 monitoring intervals over the CO_2 injection period. 13 of these monitoring samples were taken during CO_2 only injection and 15 during the WAG period.

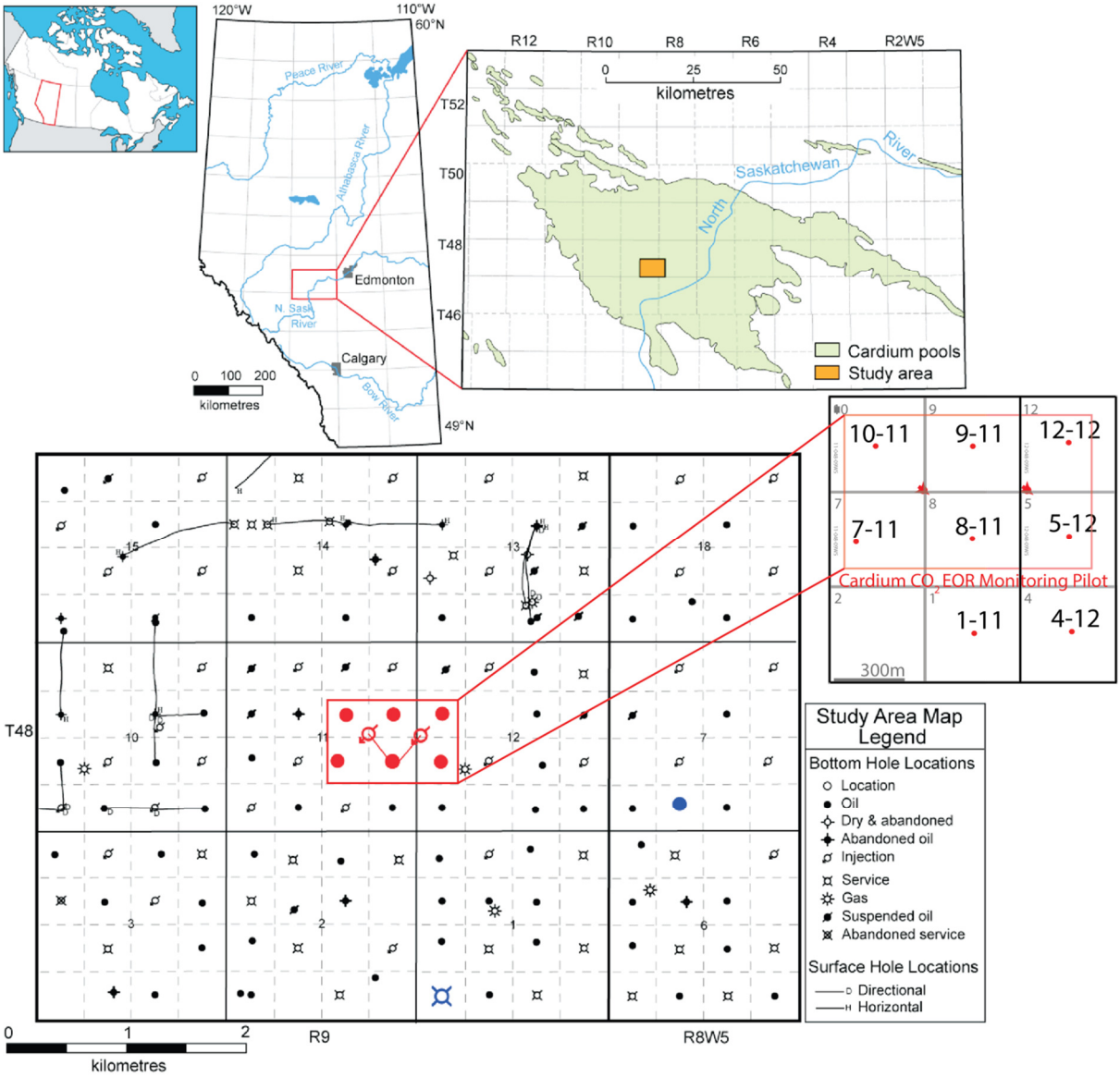

Figure 3 – Location Map of the Cardium pool, Pembina Field, adapted from (Dashtgard et al. 2008). *The Lower map illustrates the location of a wells within the study area. The 8 wells highlighted in red and expanded on the right hand side of the figure are those discussed in this report. Wells 10-11, 9-11, 7-11 and 8-11 are production wells in the classic 5 spot pattern with a CO_2 injector in the middle. Using wells 9-11 and 8-11wells 12-12 and 5-12 form a second 5 spot pattern with another CO_2 injector in the middle. Wells 1-11 and 4-12 are also production wells which sit further to the South.*

3. Assessment of trapping mechanisms from geochemical and production data

In this study two approaches to determining the relative contribution of trapping mechanisms were used. The first approach took the geochemical and production data from the two year injection interval in conjunction with solubility models to calculate the CO_2 distribution at each of the 8 sampled wells. The second approach used the stable isotope values of water sampled at the wells to calculate the phase distribution. These two approaches are described below.

Partitioning of CO_2 using geochemical and production data

Using the equilibrium solubility calculations described in section 1.3 the partitioning of CO_2 that is dissolved in the oil, brine or present as a free phase gas can be estimated for the first two years of CO_2 injection at the Pembina Cardium CO_2EOR monitoring pilot. To do this knowledge of the relatives volumes of brine, oil and CO_2 in the reservoir must also be known. At reservoir conditions the solubilites of CO_2 in brine and oil are 1.25 mol/L and 8.5 mol/L respectively. At the Pembina field monthly production volumes of gas oil and brine are available and are here used as a proxy for the relative reservoir saturations. Figure 4 shows the relative proportions of produced fluids at the Pembina Cardium CO_2EOR monitoring pilot through the first two years of straight CO_2 injection. As can be seen in the figure wells 10-11, 5-12 and 8-11 produced predominantly water over the 2 year period. Wells 1-11 and 4-12 produced similar levels of oil and water but very little CO_2. Significant volumes of CO_2 were produced at wells 7-11, 9-11 and 12-12. It must be noted that the volumes of CO_2 have units of $m^3 10^3$ and therefore the relative proportions displayed in the charts do not give an accurate representation of the real relative proportions of produced fluids in the wells that produced significant volumes of CO_2.

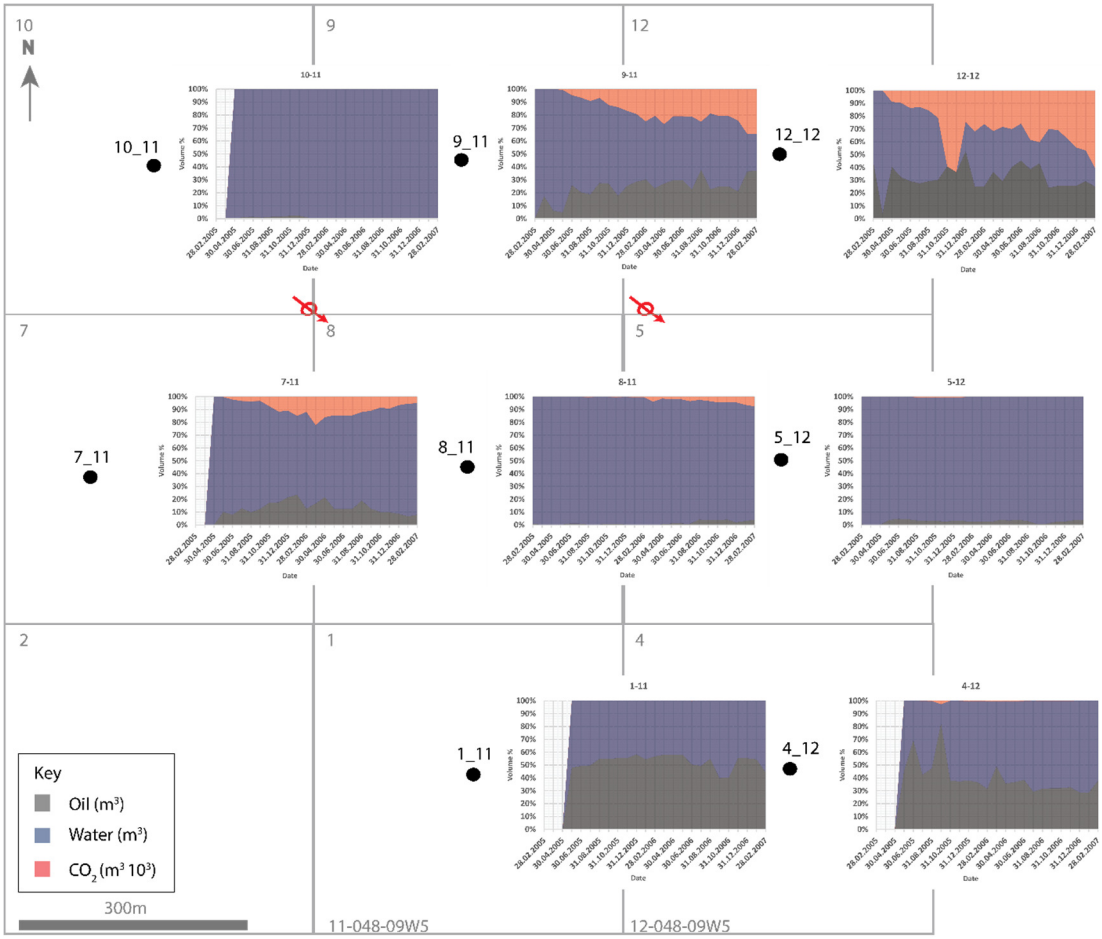

Figure 4. Produced fluids over the two year injection interval at each of the sampled wells (Data from Alberta Innovates, 2005, 2006, 2007).

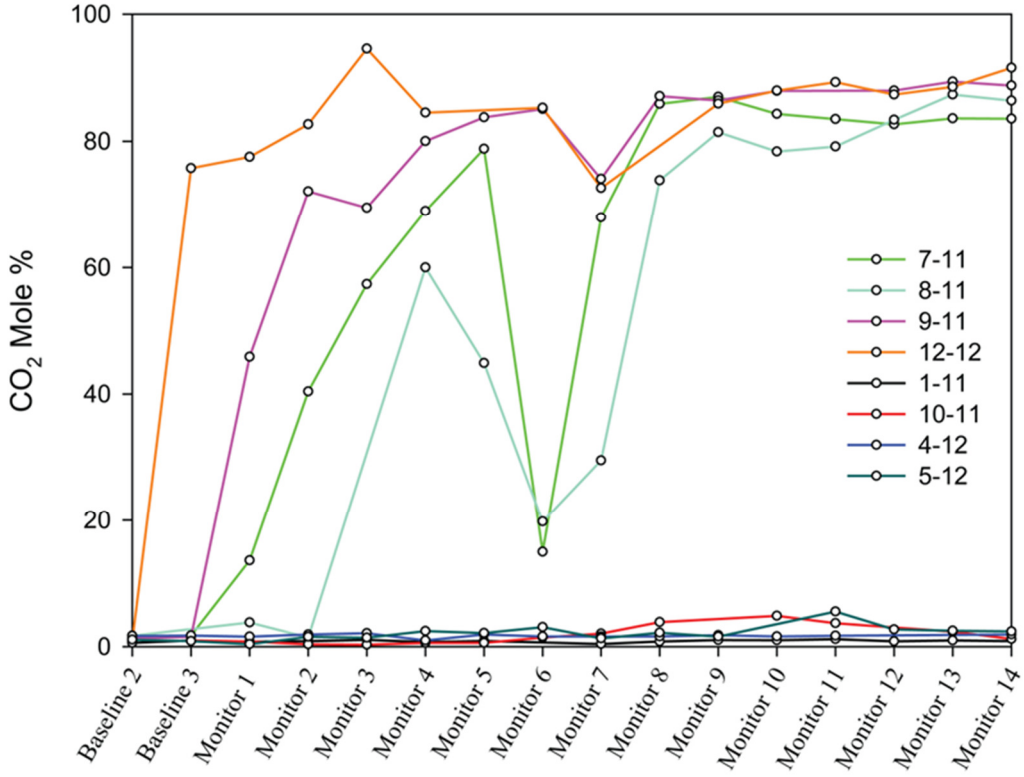

Figure 5 – CO_2 mole % of produced gas at the Pembina Cardium Monitoring Pilot during the first two years of CO_2 injection (Modified from Johnson et al., 2011a).

As observed in figure 5, the composition of produced gas changed significantly after the injection of CO_2. 3 wells 12-12, 9-11 and 7-11 (See figure 3 for location) produced CO_2 almost immediately after CO_2 injection. Well 12-12 was the first to see CO_2 with +80 mole % CO_2 in the produced gas stream after monitor 1 (baseline value 3 was sampled after CO_2 injection). An increase in CO_2 mole % at well 9-11 was first seen at Monitor 1, with values levelling at around 80 mole % by monitor 4. Wells 7-11 and 8-11 saw CO_2 later with no increase in CO_2 mole % in well 8-11 until monitor 4. These two wells also saw large decreases in CO_2 mole % around monitor interval 6. By monitor 11 wells 12-12, 8-11, 9-11 and 7-11, coined by Johnson et al. (2011a) as 'group 1 wells' all saw around 80 mole % CO_2. In contrast no increase in CO_2 mole % was observed at wells 1-11, 10-11, 4-12 and 5-12 'group 2 wells' for the entire 2 year monitor interval. Understandably the relationships observed in these wells are similar when the cumulative CO_2 flux is analysed. Wells 7-11, 9-11 and 12-12 saw cumulative CO_2 production of 157,000 297,000 and 461,000m^3 over the 2 year injection period (monitor 1-14). Well 12-12 saw the quickest increase in CO_2 flux with

cumulative 10,000m^3 after two months of injection. Wells 9-11 and 7-11 preformed similarly and took 5 months to reach the same cumulative value of 10,000m^3. CO_2 production was much slower at well 8-11 which took 13 months to reach the same cumulative value of 10,000m^3. As was highlighted by the lack of change in CO_2 mole % in wells 1-11, 10-11, 4-12 and 5-12 ('group 2' wells) there was no significant change in CO_2 flux. Over the 2 year injection period these wells saw 400, 200, 1200 and 750m^3 in wells 1-11, 10-11, 4-12 and 5-12 respectively.

Using the produced volumes displayed in figure 4 the relative mole % of CO_2 dissolved in the oil, brine and as a free phase gas was estimated for the same 2 year injection period. The equilibrium solubilities of 8.5 mol/L in oil and 1.25 mol/L in brine were multiplied by the number of litres of brine and oil produced at monthly intervals. This estimated the number of moles that would be needed to saturate both the brine and the oil. The number of moles of CO_2 in the system was calculated by multiplying the produced gas volume by the CO_2 concentration (mole %) (See figure 5) to give the volume of produced CO_2 (at well 12-12 28.02.2006 CO_2 concentration = 86.7% and produced gas = 21.14 $m^3 10^3$ therefore CO_2 produced = 18.32 $m^3 10^3$) and then dividing this number by the molecular volume of CO_2 to give the number of moles of CO_2 (18328380L / 23.64 = 775312 moles). When the number of moles of CO_2 in the system superseded the number of moles needed to saturate the brine and the oil, it was assumed that free phase CO_2 was present. When the number of moles in the system was less than number of moles needed for saturation it was assumed that both the brine and oil phase would be undersaturated with respect to CO_2. An assumption was made that the ratio of partitioning of CO_2 in brine and oil would remain constant in both under-saturated and saturated conditions. However this ratio was adjusted to represent the relative volumes of oil and brine by multiplying the saturated mole fractions by the fraction change in volume relative to a 1:1 oil water ratio. This leads to the solubility molalities (moles /L) in oil and brine remaining constant but the total number of moles in oil in relation to that in brine will be different compared to that if the oil:water ratio was 1:1. It should ne noted that the calculations used to infer the reservoir saturations from production data are only indicative because they assume that the produced fluid is representative of the average reservoir fluid, which is not generally the case.

The results of CO_2 partitioning for the first two years of CO_2 injection at the Pembina Cardium CO_2EOR monitoring pilot are displayed in figure 6. As can be seen in wells

10-11, 4-12 and 1-11, where little CO_2 was produced (See figure 6) the brine and oil are undersaturated with respect to CO_2 with no free phase CO_2 present over the two year period. In wells 4-12 and 1-11, CO_2 is partitioned into oil and brine in near equivalent molar percentages. In wells 5-12 and 10-11 CO_2 is almost entirely dissolved in brine due to the low volumes of oil and CO_2 in the reservoir over the two year injection period.

Only in wells 9-11, 12-12, 7-11 and 8-11 are significant volumes of free phase CO_2 seen. In well 12-12 the large volumes of CO_2 in the reservoir mean that by the third monitoring interval at 31.07.2005 the brine and oil are saturated with respect to CO_2 and therefore nearly 50% of CO_2 is predicted to be in free phase. Due to the increasing CO_2 production at well 12-12 an increasing proportion of CO_2 is in free phase throughout the 2 year injection period. By 28.02.2007 only around 10% of the total CO_2 is dissolved in the oil and brine. Wells 7-11 and 9-11 show similar partitioning profiles with CO_2 being predominantly dissolved in the brine and oil near the beginning of the injection period before saturation occurs and the proportion of free phase CO_2 increases. In well 7-11 however, due to decreasing volumes of produced CO_2, the proportion of CO_2 dissolved in oil and brine increases again towards the last 7 months of the two year injection period. In well 8-11 the low volume of oil means that CO_2 is predominantly partitioned into brine except at a few intervals when high CO_2 production leads to the conclusion that over 80% of the CO_2 is in free phase.

Table 1 shows the phase distribution of the CO_2 at the end of the two-year injection interval. On average across all wells 74% of the CO_2 remains as a free phase with 14% and 12% dissolved into the oil and brine phase respectively. However the range of values vary from 55-91% for CO_2 in a free phase and from 8-84% and 1-100% for CO_2 in oil and brine respectively at individual wells as described above. Thus one must be careful to not over interpret any one well in isolation of considering the production volumes.

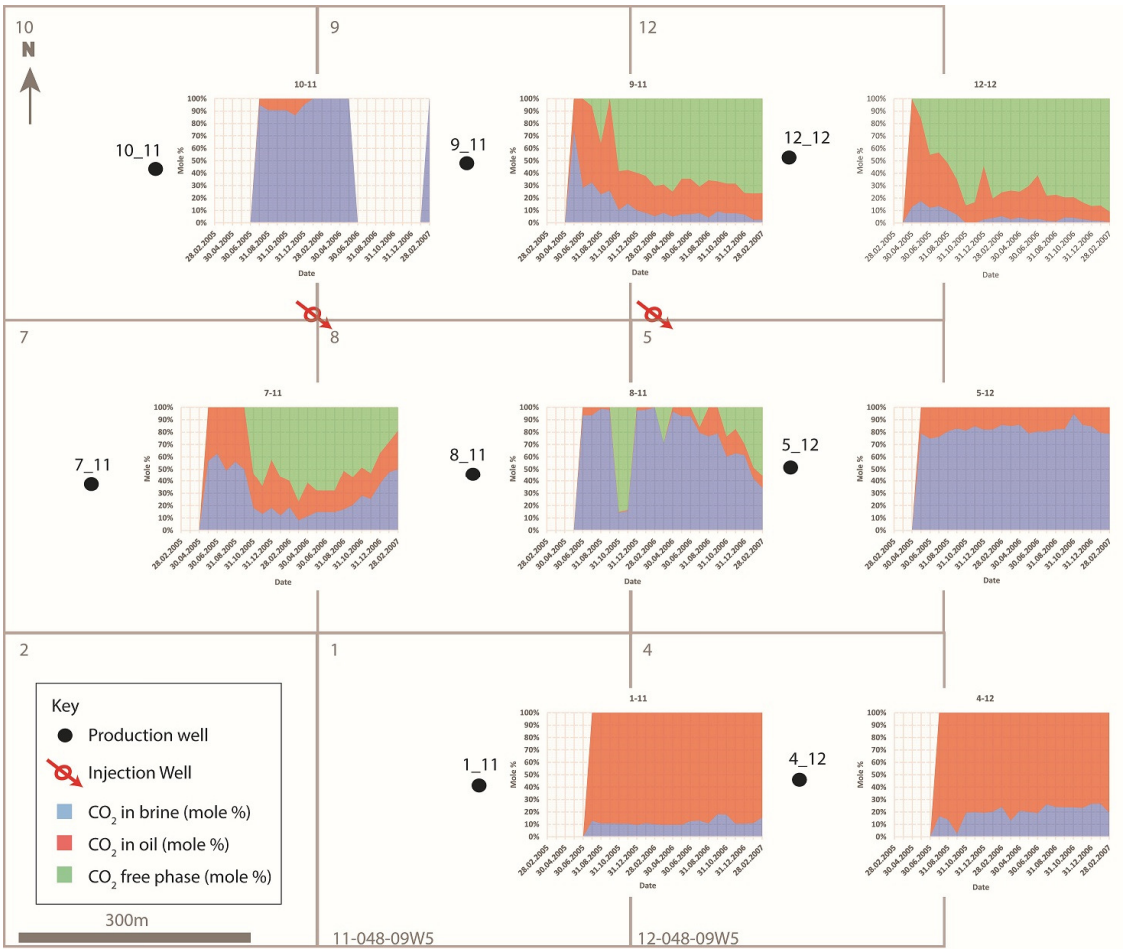

Figure 6. Mole % CO_2 in each reservoir fluid phase for each sampled well throughout the two year CO_2 injection interval calculated using production and geochemical data. Blank data indicates no gas produced thus CO_2 cannot be partitioned.

Table 1. Mole % CO_2 in each reservoir fluid phase for each sampled well at the end of the two year CO_2 injection interval.

Well	moles CO_2 in brine	as%	moles CO_2 in oil	as %	moles CO_2 free phase	as %	SUM
12_12	13163	1	156060	8	1694668	91	1863891
7_11	100100	50	61880	31	37633	19	199613
8_11	411950	34	126140	10	663962	55	1202052
9_11	30100	2	264180	21	935451	76	1229731
1_11	33	16	180	84	0	0	213
10_11	379	100	0	0	0	0	379
4_12	50	20	206	80	0	0	256
5_12	138	79	38	21	0	0	176

TOTAL	555913	608684	3331713		4496310
% Total	12	14	74		100

Partitioning of CO_2 using isotopic data

Chemical and isotopic data was obtained for baseline values (prior to CO_2 injection), during CO_2 only injection (March 2005 to January 2007) and during WAG injection (February 2007-March 2008) at the PCCMPP. Chemical analysis and isotope data for reservoir water could not be obtained when wells produced only gas or oil, or where a well had been shut in.

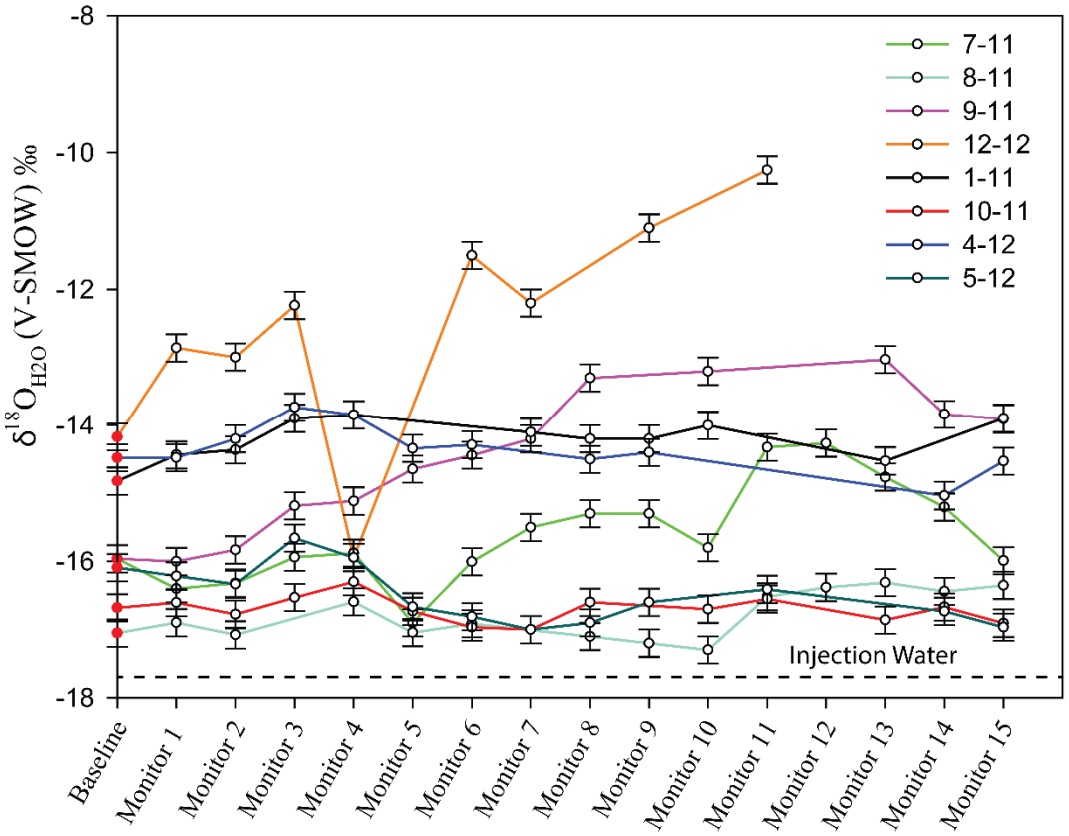

Figure 7 - $\delta^{18}OH_2O$ ‰ (V-SMOW) of produced reservoir water over the first two years of CO_2 injection at the Pembina Cardium CO_2EOR monitoring pilot. The $\delta^{18}O$ value of injection water is shown by the dashed line. Baseline $\delta^{18}O$ values for each well are shown by red circles (Data from Alberta Innovates, 2005, 2006, 2007).

The $\delta^{18}O$ of reservoir waters through the 2 year injection period are displayed in figure 7. Where circles are present at monitor intervals $\delta^{18}O$ data was available. Trends are extended between sampling points where no data exists due to the lack

of produced water. Baseline values of $\delta^{18}O$ at each well are shown by red points on Figure 7. Baseline values vary from ~17 to 14 ‰ which corresponds to a value that is a mixture between meteoric water used for the water flood (approximately -20‰) and the original formation water (-10‰) (Johnson et al., 2011b and references therein). Plotting both the $\delta^{18}O$ and $\delta^{2}H$ values of the baseline waters with historic water flood and original formation waters shows a clear mixing trend between the two end-members with some wells showing a greater influence of meteoric water than others (Johnson et al., 2011b). Well 12-12 showed the largest variation from baseline with a maximum increase of 3.95‰ compared to baseline values over the two-year injection period. Well 9-11 saw the second largest increase in $\delta^{18}O$ with a maximum increase of 2.8‰ at monitor 10. In the following monitor periods $\delta^{18}O$ values still increased but by a smaller amount. Well 7-11 saw an increase of $\delta^{18}O$ values of reservoir water with a maximum increase of 1.74‰ compared to baseline at monitor 12. Monitor periods 13, 14 and 15 however showed less of an increase in $\delta^{18}O$. Smaller increases of $\delta^{18}O$ were observed at 8-11 where a maximum increase of 0.74‰ was observed at monitor period 13. Small increases were also seen at well 1-11 with a maximum change in $\delta^{18}O$ of 0.96‰ at monitor 4 before remaining constant for the remainder of the 2 year injection period.

In contrast wells 10-11, 4-12 and 5-12 showed no increase in $\delta^{18}O$ values of produced water during the 2 year CO_2 injection period. At 10-11 and 4-12 $\delta^{18}O$ values remained constant within the measurement uncertainty. At well 5-12 $\delta^{18}O$ values decreased at a maximum value of -0.91‰ at monitor 7.

As described by Johnson et al. (2011b), in most natural environments the amount of oxygen in CO_2 is extremely small compared to the amount of oxygen in H_2O. This means the oxygen isotope ratios of the water remain near constant and the oxygen isotope ratios of the CO_2 take on the value of H_2O (plus the appropriate isotope enrichment factor depending on the temperature and salinity). However at CO_2 injection sites, CO_2 may become a large source of oxygen, causing the isotope ratios of the H_2O and CO_2 to change if the injected CO_2 has a distinct isotope signature. Based on work by Lécuyer et al. (2009), Johnson et al. (2011b) suggest that this isotopic exchange, the rate of which is dependent on salinity and temperature, will occur within a matter of hours at the temperatures and salinities of the Pembina field (50^0C and $5g\ L^{-1}$). To assess the relative contribution of oxygen isotope ratios from CO_2 and H_2O, two end member values must be established. At the Pembina field prior to CO_2 injection isotope ratios of the CO_2 water system will be controlled by the

water. The water at the Pembina field has an isotopic signature of -17.0 to -14.2 ‰. However if the isotope ratio of the CO_2-water system takes on that of injected CO_2, as might happen around the injection well, it will have isotopic values nearer to that of the injected CO_2 which has a $\delta^{18}O$ value of +28.6‰. The resultant $\delta^{18}O$ value of the reservoir water that has been in contact with injected CO_2 can be calculated by the following equation:

$$\delta^{18}O^{f}_{H_2O} = \left(\delta^{18}O^{i}_{H_2O} * \left(1 - X^{0}_{CO_2}\right)\right) + X^{0}_{CO_2}(\delta^{18}O_{CO_2} - \varepsilon) \quad [1]$$

where the superscripts i and f refer to initial and final conditions respectively, ε is the isotope enrichment factor for CO_2–water at 50 ℃ (35.5‰) and $X^{0}_{CO_2}$ is the fraction of oxygen in the system sourced from the CO_2. Therefore any changes in $\delta^{18}O$ value of the reservoir water, induced by CO_2 injection would cause the $\delta^{18}O$ value to increase, with a theoretical maximum of ~ -7 ‰ (Johnson et al., 2011b). Using the equation:

$$X^{0}_{CO_2} = \frac{AS_{CO_2} + BS_w}{AS_{CO_2} + BS_w + CS_w} \quad [2]$$

where A= moles of oxygen in 1L of free phase CO_2, B= moles of oxygen dissolved in 1L of water from CO_2 and C = moles of oxygen in 1L H_2O, Johnson et al. (2011b) estimated that in a fully CO_2 saturated water system that only ~4% of the oxygen can be sourced from dissolved CO_2. This would lead to a maximum 0.4‰ shift in the $\delta^{18}O$ value of produced water at the Pembina field (with baseline values of $\delta^{18}O_{H20}$ = -16‰ and $\delta^{18}O_{CO2}$ = +28.6). The solubility of CO_2 in H_2O used within this equation is based on Duan & Sun's (2003) CO_2 solubility equation which, under Pembina reservoir conditions (50^{0}C, 19Mpa, 0.086 M NaCl) gives an estimate of 1.27 mol L^{-1}. As Johnson et al. (2011b) indicates, this contributes 2.52 mol of oxygen (parameter B in equation 2) to a litre of CO_2 saturated water which has 55.51 mol of oxygen initially present (parameter C in equation 2). Therefore any free phase CO_2 (parameter C in equation 2) would have the ability to shift the $\delta^{18}O_{H2O}$ beyond the dissolved CO_2 change of +0.4‰. Johnson et al. (2011b) suggest that at Pembina, free phase CO_2 filling the available pore space would have the ability to cause a maximum shift in $\delta^{18}O_{H20}$ of +9‰. Using this theory Johnson et al. (2011b) suggest that the magnitude in change of the $\delta^{18}O_{H20}$ over the value of CO_2 saturation can then be used to estimate the relative proportions of CO_2 and H_2O in the system. This can be done by rearranging equation x to give:

$$X^0_{CO_2} = \frac{\delta^{18}O^i_{H_2O} - \delta^{18}O^f_{H_2O}}{\delta^{18}O^i_{H_2O} + \epsilon - \delta^{18}O_{CO_2}} \quad [3]$$

which allows the fraction of oxygen in the reservoir sourced from CO_2 to be calculated ($X^0_{CO_2}$), which for example at well 12-12 Monitor Interval 6:

$$X^0_{CO_2} = \frac{-14.17 - -11.51}{-14.17 + 35.5 - 28.6} = 0.37$$

Johnson et al. (2011b) do however note that this method assumes no density driven convective overturn or admixture of oxygen from other sources. From this CO_2 saturation can be estimated assuming $S_{CO2} + S_{H2O} = 1$.

$$S_{CO_2} = \frac{BX^0_{CO_2} + CX^0_{CO_2} - B}{A - B - AX^0_{CO_2} + BX^0_{CO_2} + CX^0_{CO_2}} \quad [4]$$

Which again for well 12-12 monitor interval 6:

$$S_{CO_2} = \frac{2.52\ (0.37) + (55.51)0.57 - 2.52}{35.65 - 2.52 - 35.65(0.37) + 2.52(0.37) + 55.51(0.37)} = 0.45$$

therefore implying that the pore space at well 12-12 at monitor interval 6 is comprised of 0.45 CO_2 and 0.55 H_2O. This method was applied to all 8 wells at the Pembina Cardium CO_2EOR monitoring pilot at each monitoring interval over the first two year injection period. The results are displayed in figure 8. As can be seen maximum CO_2 fractions are observed in well 12-12 with a relatively linear increase to a maximum of 0.64 CO_2 at monitor period 11. A linear increase in CO_2 fractions were also observed in well 9-11 with up to 0.4 CO_2 at monitor 13. An increase in CO_2 fraction was not observed in well 7-11 until monitor period 11 and reached a peak of 0.22 CO_2 at monitor 12. At well 1-11 a CO_2 fraction of 0.13 was reached after monitor period four but was followed by a steady decrease in CO_2 fraction over the remainder of the 2 year interval until a small increase again at monitor 15. Although well 4-12 saw a CO_2 fraction 0.09 at monitor 3, wells 4-12, 5-12 and 10-11 generally saw CO_2 fractions of 0 over the two year injection period. This method assumes that there is only CO_2 and H_2O in the pore-space i.e. a two component system, and does not consider both the CO_2 that may be dissolved in an oil phase and the oil phase itself.

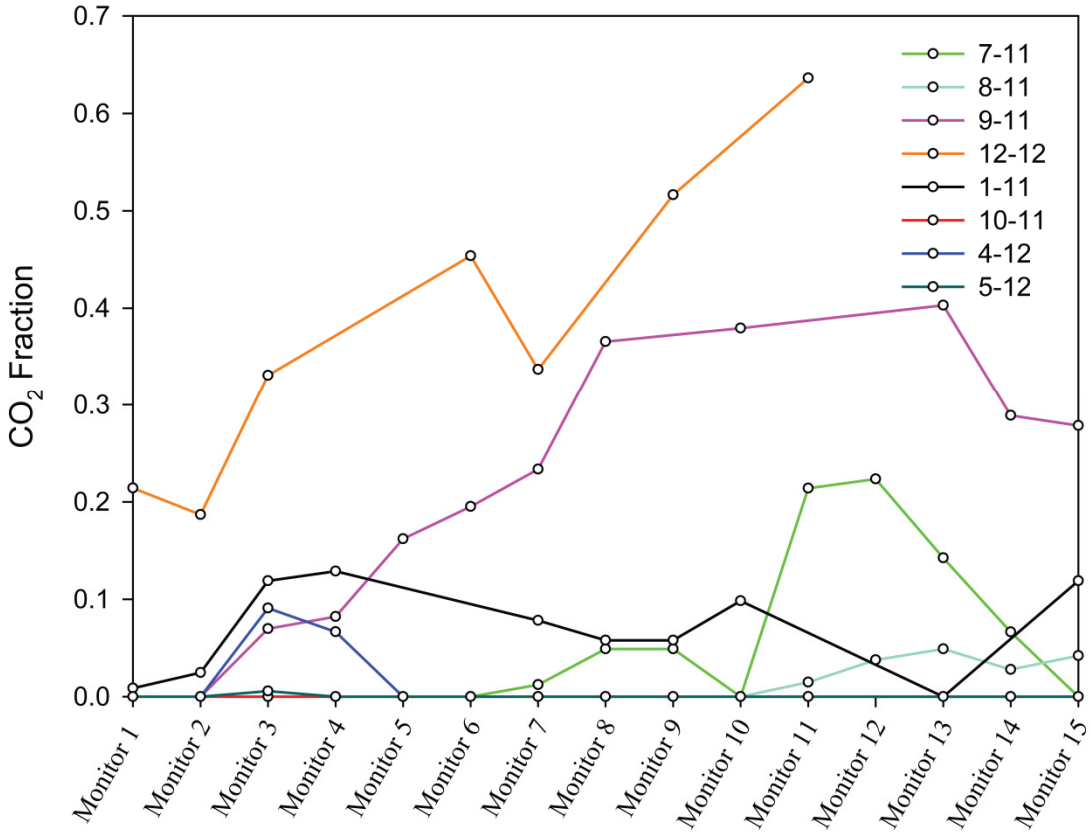

Figure 8 – Isotopically derived CO_2 fractions predicted at each monitor interval for the first two years of CO_2 injection at the Pembina Cardium Monitoring Project. This method assumes a two phase system and therefore fractions represent the pore space occupied only by water and CO_2.

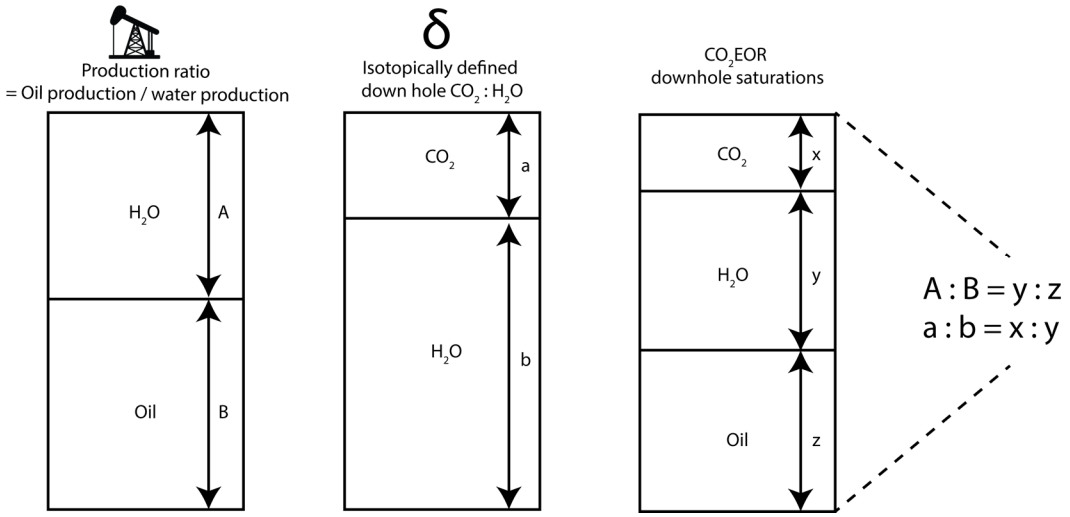

Figure 9 – Schematic representation of method used to correct CO_2:H_2O fractions to allow for an oil phase.

Correcting pore space saturations for oil phase

As explained above, shifts in $\delta^{18}O$ of produced reservoir water can be used to predict the relative fractions of free phase CO_2 and H_2O in a reservoir. However this method does not account for an oil phase, which in certain reservoirs, will account for a proportion of the pore space and may also hold dissolved CO_2 (Stalkup, 1978).

Therefore to fully understand the downhole CO_2 saturation, the CO_2 fraction calculated by the $\delta^{18}O$ isotope method must be corrected to account for an oil phase. This was completed using both the oil : H_2O production ratio (B:A in figure 9) and the isotopically derived CO_2 : H_2O ratio (a:b in figure 9). Oil volumes were corrected from surface volumes to reservoir volumes using a formation volume factor of 1.2 (Clarkson & Pedersen 2010). As both ratios represent volumes it can be assumed that the ratio of CO_2 : H_2O, taken as pore space fraction, can then be used to calculate a representative pore space fraction for oil based on the oil : H_2O production ratio. These fractions can then be summed and a fraction of total pore volume for each can be calculated. For example in well 12-12 at monitor period 6:

The oil: H_2O production ratio (B:A) = 38 : 62

The isotopically defined CO_2 : H_2O ratio (a:b) = 0.45 : 0.55

Therefore the oil proportion relative to the CO_2 : H_2O ratio = 0.55 * 38/62 = 0.34

So the relative proportions of oil : CO_2 : H_2O = 0.34 : 0.45 : 0.55

Which when normalized to equal 1 equates to 0.25 : 0.34 : 0.41 as pore space fractions. (z:y:x in figure 9)

Therefore accounting for the fraction of oil in the reservoir, at well 12-12 monitor period 6, S_o = 0.25, S_{CO2} = 0.34 and S_w = 0.41. This method was used to correct S_{CO2} and S_w values at all wells at each monitoring interval over the two year injection period.

Pore space saturations were subsequently converted to Mole % of CO_2 by calculating the number of moles for a given pore fraction (as already determined) in each phase where CO_2 is present. To do this the solubilities of 1.25 and 8.5 mol/L were used for the brine and oil phases respectively and a density of 0.77kg/L for the gas phase for CO_2 when present. The resulting corrected values for CO_2 distribution between the reservoir phases at each well is shown in figure 10.

Figure 10. Mole % CO_2 in each reservoir fluid phase for each sampled well throughout the two year CO_2 injection interval calculated using isotopic data. Blank data indicate where isotopic approach does not calculate a free phase CO_2.

Comparison of production and isotopic data approaches

Results in figures 6 and 10 for the two approaches described above to calculate relative contributions of trapping mechanisms are broadly similar but do show some differences. Table 1 shows that for the geochemical and production data approach that after two years on average 74% of the CO_2 remains as free phase with 14 and 12 % of the CO_2 dissolved in the oil and brine respectively. Similar calculations for the isotopic approach can be made but in some cases will not match as the isotope approach only works where a free-phase CO_2 is present. This is because the method works by assuming fluid saturation. Thus in wells where there is no free phase CO_2 no estimate of CO_2 partitioning has been made. In reality as highlighted by the production method approach CO_2 may be dissolved in the reservoir fluids without saturating them. However in wells where free phase CO_2 is predicted such as 8-11, 7-11, 12-12 and 9-11 similar partitioning trends can be seen throughout the two year injection period (compare Fig 6 and Fig 10). Although variations exist, the similarity of results using the two different methods gives confidence that the CO_2 partitioning results may be representative.

.

4. Reservoir Modelling

An "approximative" compositional reservoir simulation model of the Pembina Cardium CO_2 Monitoring Pilot Project (PCCMP) located in west-central Alberta, Canada. The primary purpose of the model developed here was not to match any project specific injection and production history (without more resources this would have not been possible anyway), but rather to use it as a test-bed to investigate various CO_2 injection scenarios with a model having some of the salient features of the pilot project. In particular, the question posed was the differentiation between the proportions of CO_2 that is dissolved in water and CO_2 dissolved in oil, as well as CO_2 in the mobile and residual in the free gas phase, under various injection scenarios, such as could be reasonably envisaged for such a site.

A secondary objective of the work was to utilize the output from the model to provide a calibrated pore space saturation of reservoir fluids for a two year CO_2 injection period in a CO_2-EOR pilot for comparison with the geochemical models developed as part of this work package. In the absence of an available underlying Petrel or other software geological model, the reservoir simulation model was developed from data available in Hitchon (2009) and reports published by the trial operator (Penn West, 2005, 2006 & 2007).

Model development

The model was developed using CMG[1] GEM compositional reservoir simulation software. Although the CO_2-EOR pilot was originally set up with two CO_2 injection wells in two five-spot patterns, the pilot area had been previously extensively water-flooded for approximately 50 years prior to the commencement of CO_2 injection. The well density and spacing for the water-flooding had had no definitive well pattern but was nominally an inverted 9-spot on a 40 acre well spacing, although there were also some injectors set up in line drive pattern. The CO_2 injectors were then further incorporated at the trial site in two five-spot patterns. These well patterns are illustrated in figures 3 and 11.

[1] Computer Modelling Group http://www.cmgl.ca/software/gem2014.

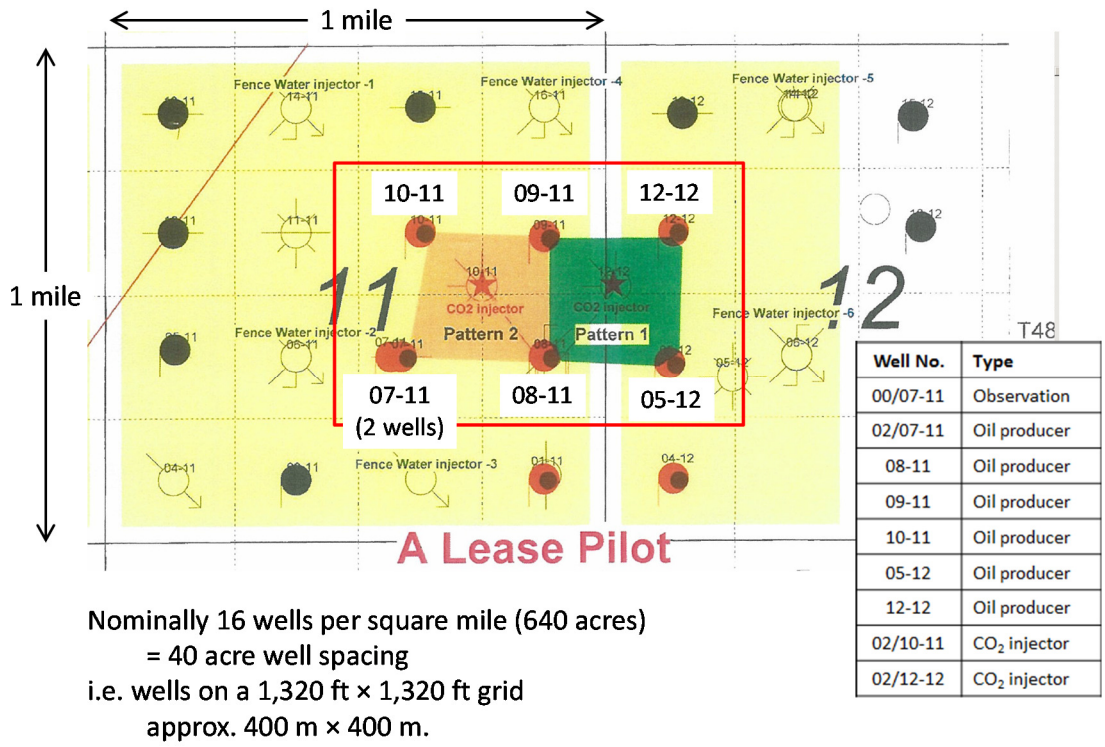

Well No.	Type
00/07-11	Observation
02/07-11	Oil producer
08-11	Oil producer
09-11	Oil producer
10-11	Oil producer
05-12	Oil producer
12-12	Oil producer
02/10-11	CO_2 injector
02/12-12	CO_2 injector

Figure 11. Layout of wells at the CO_2-EOR pilot site

Details of the reservoir lithology at the actual trial site are described in various locations in Hitchon (2009). An example from one well in the Cardium formation is shown in figure 12. Although not one of the pilot site wells, the significant details to be taken from this figure are the differentiation and placing of the various rock types typically present in the Cardium formation. From a description given of formation unit thicknesses and cross-plots of petrophysical properties at the site – see figure 13, a table – see table 2, of petrophysical properties was assembled for the model.

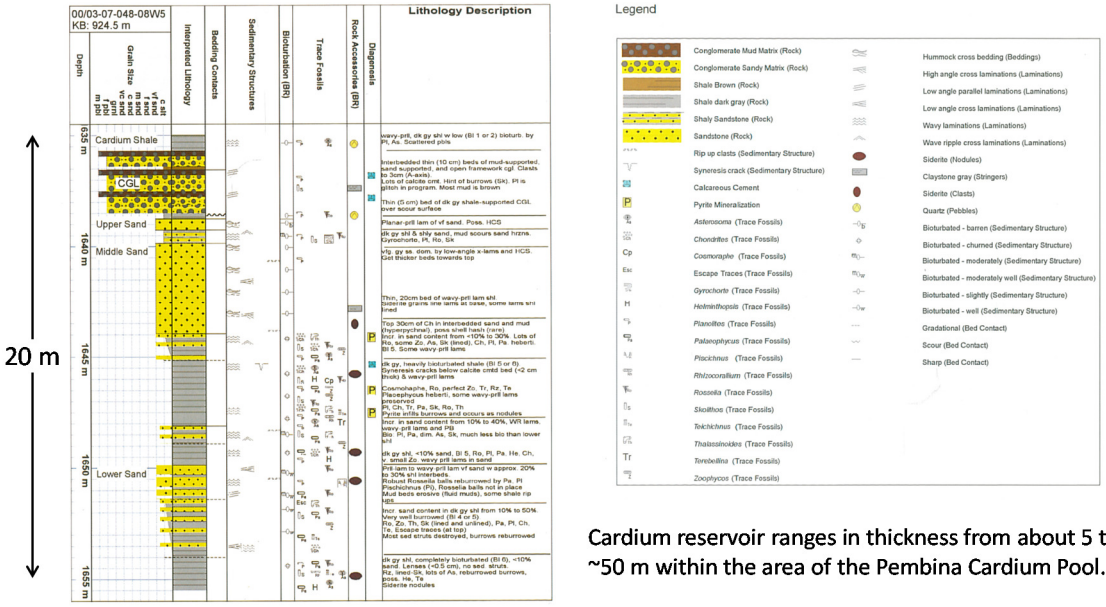

Cardium reservoir ranges in thickness from about 5 to ~50 m within the area of the Pembina Cardium Pool.

Figure 12. Example of Cardium reservoir lithology in the Pembina Cardium Pool.

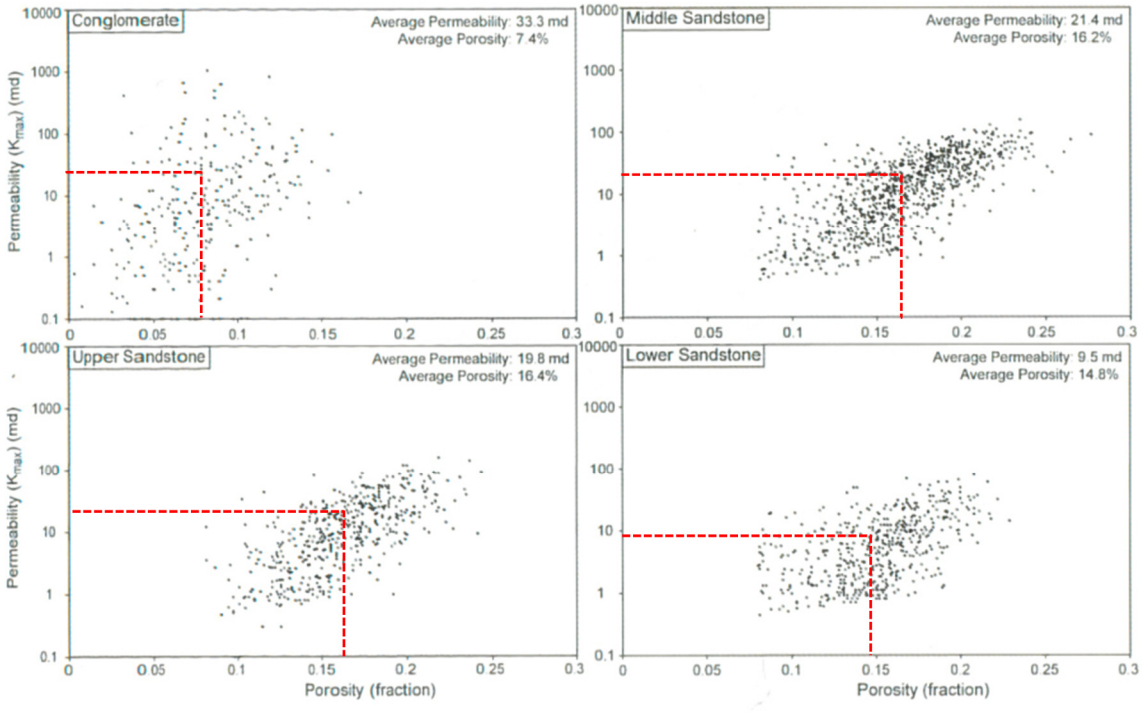

Figure 13. Porosity-permeability cross-plots for net pay in the Cardium Formation (red dashed lines indicate average values of data points).

Table 2. GEM model layer properties.

Description	Thickness m	Layer range	Porosity %	Permeability mD	k_v/k_v ratio
Conglomerate	1	1	7	33	0.2
Upper sandstone	3	2 → 4	16	20	0.2
Shale	1	5	1	0.01	0.2
Middle sandstone	3	6 → 8	16	20	0.2
Shale	5	9 → 12	1	0.01	0.2
Lower sandstone	3	13 → 15	14	10	0.2

The model was constructed with a 21 × 21 × 15 grid with 20 m × 20 m cells in the areal plane. Initially the model was assumed perfectly horizontal, but later a NE-SW trending dip angle was incorporated into the model geometry to replicate the dip angle at the site. The initial wells were located at the four corners of the model, with 3 producers at the NW, NE and SE corners and a water injector at the SW corner. The CO_2 injector was located in the centre of the model. This well pattern was an approximative representation of the actual well pattern and was only intended to capture the salient features of the projected water/CO_2 floods. It was not intended to be a one-to-one representation of the pilot wells. Well geometry fraction factors of 0.25 were applied to the wells at the corners of the grid boundary as they modelled only a quarter of a circle that the well models. The assembled model grid is shown in figure 14. Note that the reservoir layers were homogeneous.

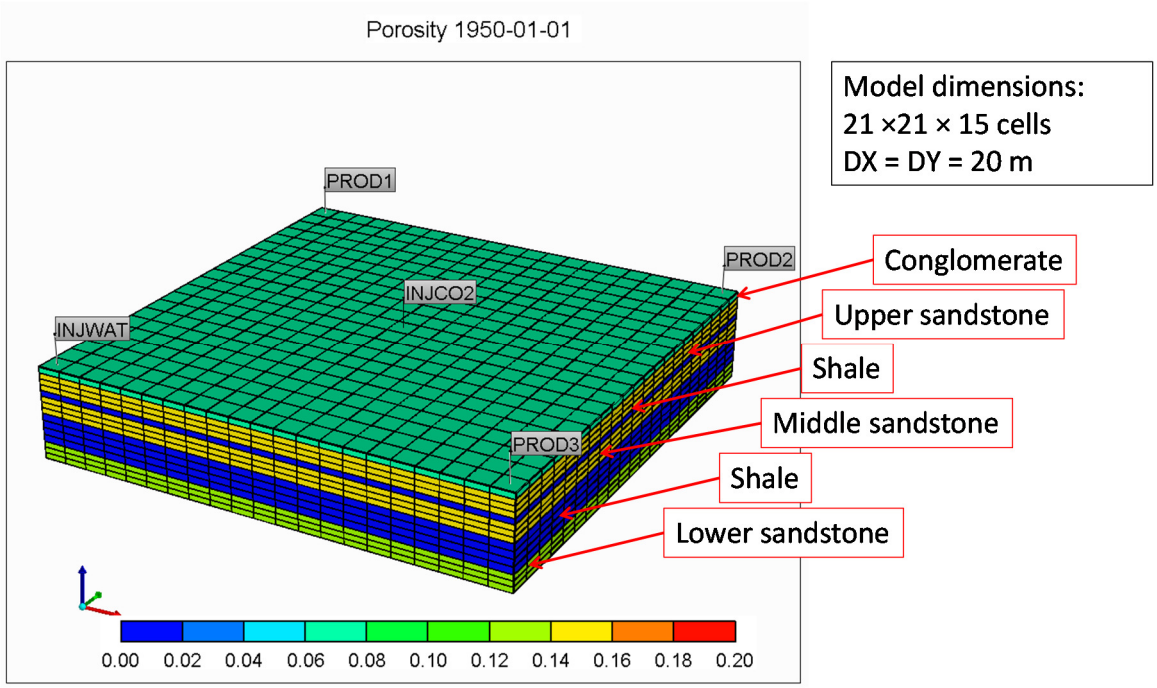

Figure 14. GEM model grid showing porosity differentiated layers.

Very little data is given in the various PCCMP reports regarding the native oil PVT properties. However, phase behaviour characterization is given from laboratory tests carried out on recombined samples with varying proportions of CO_2 (solvent) mole %. These are presented for the 0% CO_2 mole fluid in table 3. In the absence of any other suitable data it was decided to utilize the PVT data from a CMG CO_2-EOR WinProp/GEM training tutorial for this, (CMG, 2014). This fluid was a lumped 7-component model with a composition given in table 4. The data for this model had been developed in WinProp in field units. It was re-exported from WinProp in SI units at the Cardium reservoir temperature of 53℃. The minimum miscibility pressure (MMP) of this oil had been matched to a laboratory determined value of approximately 2510 psi (17.31 MPa).

Table 3. Trial site fluid properties (from recombined fluid samples with CO_2 mole 0%).

Property	Value	Units
Density	0.7188	g/cm^3
Viscosity	0.6320	mPa.s
Formation Volume Factor	1.3253	
Solution Gas-Oil Ratio	124.60	m^3/m^3
Bubble-point Pressure	16.97	MPa

Table 4. Fluid model components.

Component name		Fraction %
1	CO2	1.2
2	N2 to CH4	11.7
3	C2H6 to NC4	19.5
4	IC5 to C7	22.0
5	C8 to C12	28.2
6	C13 to C19	9.4
7	C20 to C30	8.1

The solubility of CO_2 (and the other hydrocarbon components) dissolved in water was calculated using Henry's Law with Harvey's correlation used for CO_2 Henry's constant which makes the constant a function of pressure, temperature and salinity (Harvey, 1996). For the simulations reported here the water salinity was taken to be zero.

More convenient rock-fluid (or relative permeability data) is provided in Hitchon (2009). A plot of water, oil and gas relative permeability curves used in the reservoir modelling described in the report was readily reproduced in CMG Builder software, as illustrated in figure 15.

The model was initialized with a pressure of 18.5 MPa at a depth of 1625 m (the assumed reservoir top at the CO_2 injector location. The water/oil contact depth was set at 1725 m (well below the reservoir base) to ensure an oil column which was taken to have an initial composition as given in table 4.

(a)

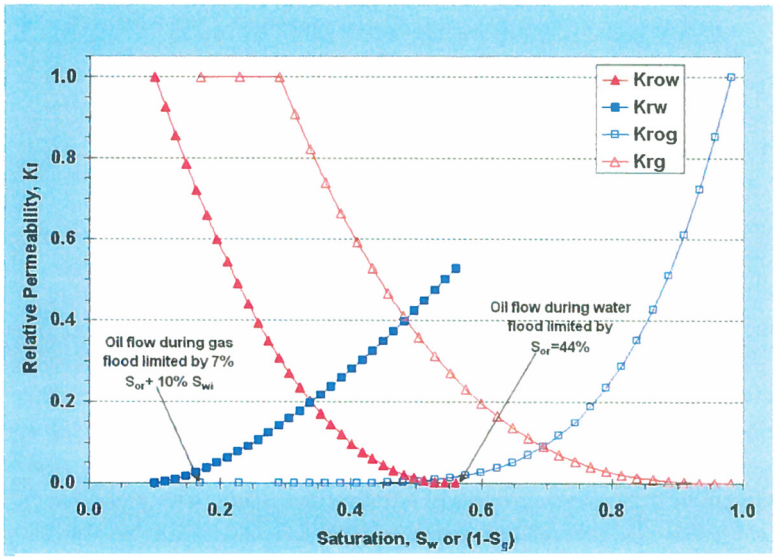

(b)

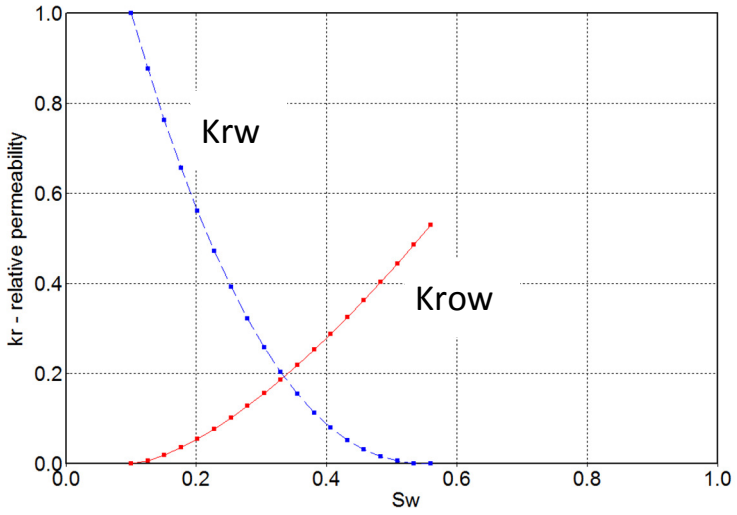

(c)

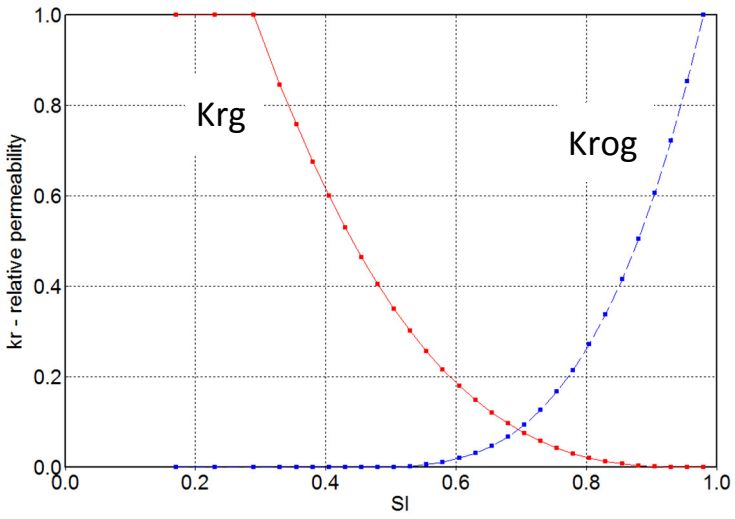

Figure 15. Comparison of relative permeability curves given in the PCCMP report (a) and Builder generated curves for water (b) and gas (c).

4.1 Initial simulation

As indicated previously the model was initially set up with 3 producers and 2 injectors and run to simulate the operation of the PCCMPP (Case 0). The model was run as an initial water-flood simulation for 50 years followed by a restarted CO_2 injection period, then all wells were shut in and an equilibration period simulated. For the sake of simplicity the simulation was commenced on 1st January 1950, so that the CO_2 injection commenced on 1st January 2000. These dates do not correspond exactly to the actual pilot dates but were chosen for notional presentation purposes. During the water-flood the producers were each set to liquid production at a rate of 2 m^3/day and the water injector set to voidage replacement by group control with the producers. The progression of the water-flood is illustrated in figure 16, where a diagonal cross-section through the model from the NE to SW corners, intersecting the water injector, CO_2 injector location (to be opened) and the producer furthest from the water injector, is shown.

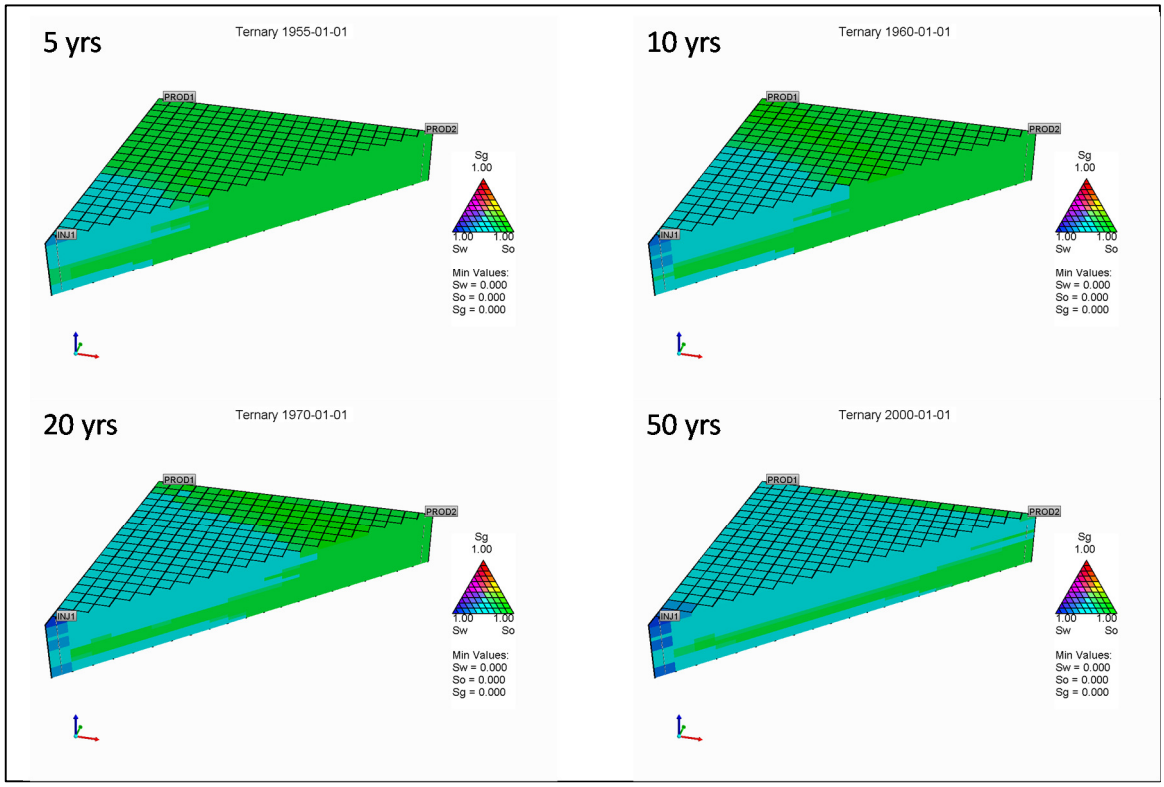

Figure 16. Ternary plots of water-flood simulation results (Case 0).

The water-flood simulation was then followed by a 2 year phase of CO_2 injection, the water injector being shut in and the producers continuing to flow at the same previous rates. The well constraint for the CO_2 injector was set as a WBHP target of

20 MPa. The progression of the CO_2 injection phase is illustrated in figure 17 with further ternary plots at the diagonal cross-section.

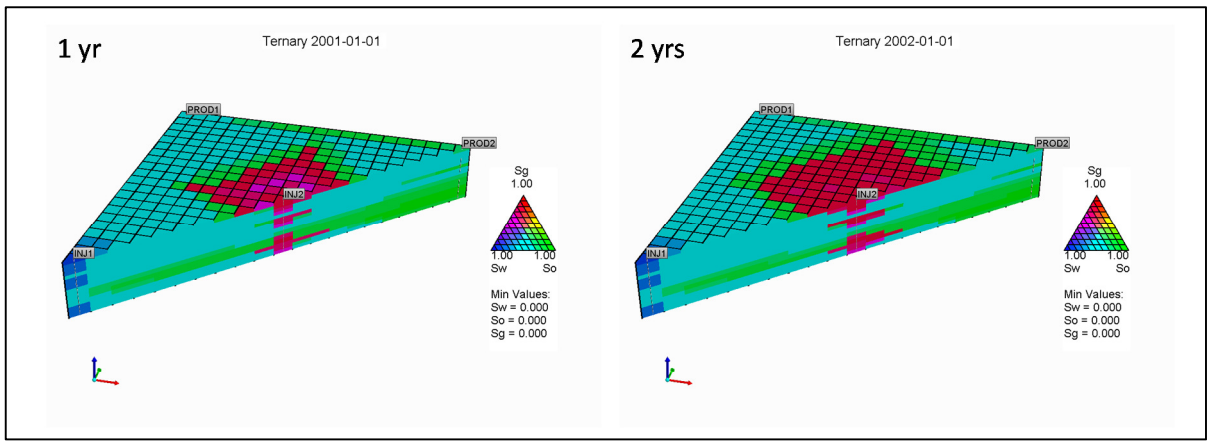

Figure 17. Ternary plots of CO_2 injection simulation results (Case 0).

For the final phase of the simulation where the system was allowed to equilibrate, all wells were shut in and the simulation continued for a further 498 years to 1st January 2500. The simulation results illustrating the partition of CO_2 moles in the water, oil and gas phases and field pressure over water-flooding, CO_2 injection and equilibration are shown in figure 18.

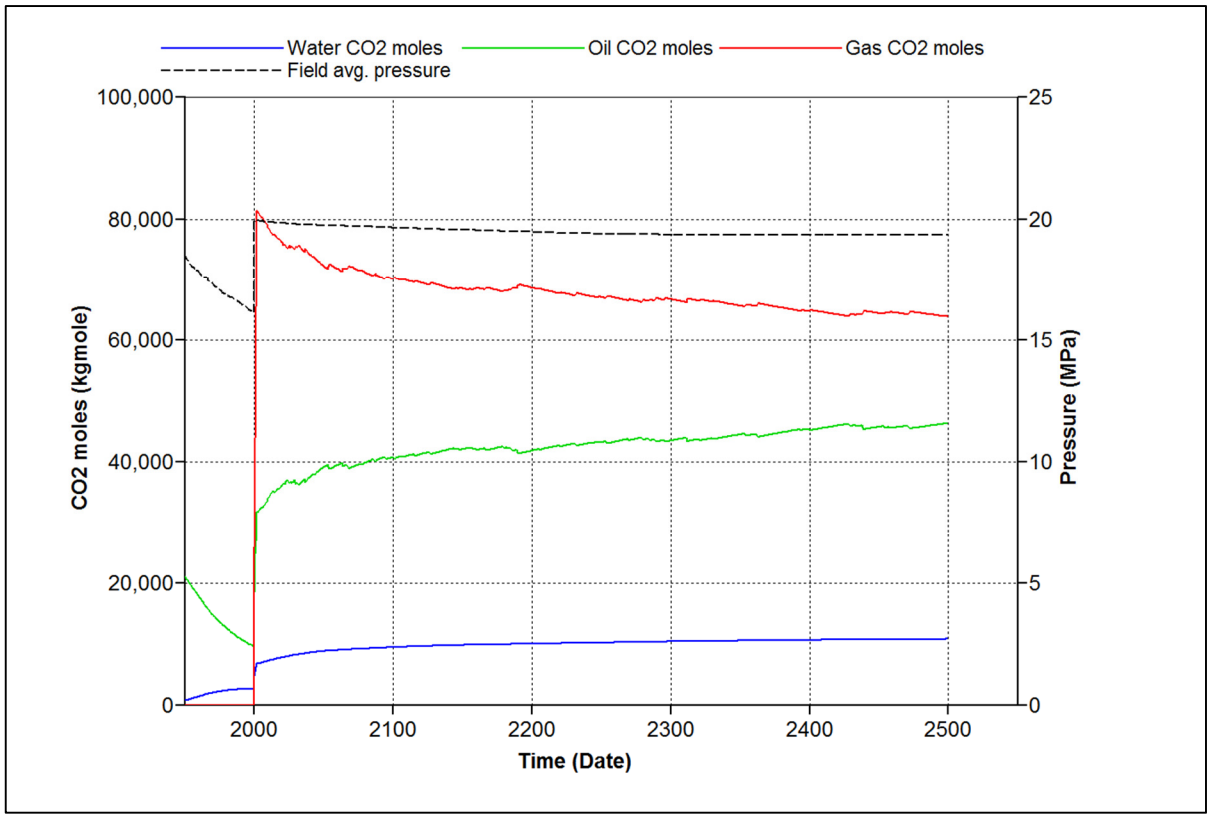

Figure 18. Initial simulation results showing the partition of CO_2 moles in the water, oil and gas and field pressure over water-flooding, CO_2 injection and equilibration phases (Case 0).

Following a review of the modelling, a small dip angle was introduced to the model geometry. This consisted of a dip angle of 0.57° orientated along the diagonal from the NE to SW corner (with the SW corner deeper than the NE corner). The effect of this small angle was hardly noticeable on fluid migration over the dimensions of the model and time-scales modelled here.

The final post CO_2 injection (2002 in figure 18) CO_2 distributions were 68% in the free (gas) phase, 26% in the oil phase and 6 % in the water phase. This compares to an average of 74% in free phase, 14% in the oil phase and 12% in the water phase at the wells sampled during the operations (See table 1) which is considered a good fit given the uncertainty in the oil:water ratio at the start of CO_2 injection.

4.2 Further simulations

The model was then run in four separate configurations (referred to as 'Cases'):

1. Continuous CO_2 injection for 5 years following 50 years water-flood.
2. Water alternating gas (WAG) injection on a 3 months cycle for 5 years following 50 years water-flood.
3. As a depleted oil field for 5 years following 50 years water-flood.
4. As an aquifer with continuous CO_2 injection for 5 years.

The CO_2 injection phase of the simulations was generally performed by restarts of the water-flood phase. Each simulation was then followed by a 45 years equilibration period, with all wells shut in.

For the WAG case two co-located injection wells were set up – one a CO_2 injector and the other the water injector – so that the injected fluid could be readily cycled between water and CO_2. In this case the well constraints were set up as reservoir volume injection rates of 8 rm^3/day. For the depleted oil field case the constraints were changed to a surface rate of 2500 sm^3/day which was equivalent to the surface CO_2 injection rate in the continuous gas injection case. For the aquifer case, the reservoir model was set up with the same fluid model except the model was initialized with the oil-water contact well above the reservoir top and with a composition with a very small fraction of CO_2, the fraction of the 'N2 to CH4' component being correspondingly increased. Since there are no hydrocarbons present in the system, this corruption of the fluid model data is immaterial to the simulation results. The producers were kept open and flowing for this simulation to simulate losses to the aquifer. However for the depleted oil field case the producers were shut in. The well constraints for the various cases are summarised in table 5.

Case	Scenario	Water-flood phase		CO_2 Injection phase		Equilibration phase	
		Duration (years)	Well constraints	Duration (years)	Well constraints	Duration (years)	Well constraints
0	Continuous gas injection	50	Producers: liquid rate 2 sm^3/day Injector: group voidage replacement	2	Producers: liquid rate 2 sm^3/day Injector: WBHP 20 MPa	498	All wells shut in
1	Continuous gas injection	50	Producers: liquid rate 2 sm^3/day Injector: group voidage replacement	5	Producers: liquid rate 2 sm^3/day Injector: res. rate 8 rm^3/day	45	All wells shut in
2	Water alternating gas	50	Producers: liquid rate 2 sm^3/day Injector: group voidage replacement	5	Producers: liquid rate 2 sm^3/day Injectors: CO_2 res. rate 8 rm^3/day Water surf. rate 8 sm^3/day on 3 month cycle	45	All wells shut in
3	Depleted oil field	50	Producers: liquid rate 2 sm^3/day Injector: group voidage replacement	5	Producers: shut in Injector: Surface rate 2500 sm^3/day	45	All wells shut in
4	Aquifer injection	N/a	N/a	5	Producers: liquid rate 2 sm^3/day Injector: res. rate 8 rm^3/day	45	All wells shut in

Table 5. Summary of modelled cases.

The simulation results illustrating the partition of CO_2 moles in the water, oil and gas over water-flooding, CO_2 injection and equilibration phases for these cases are shown in figures 19-22. Also shown in these plots is the corresponding field pressure during the simulations. The data from these plots was exported to Excel, and charts showing the relative proportions of CO_2 kg moles in the water, oil and gas phases over the 45 years equilibration period after which injection ceased are shown in figure 23.

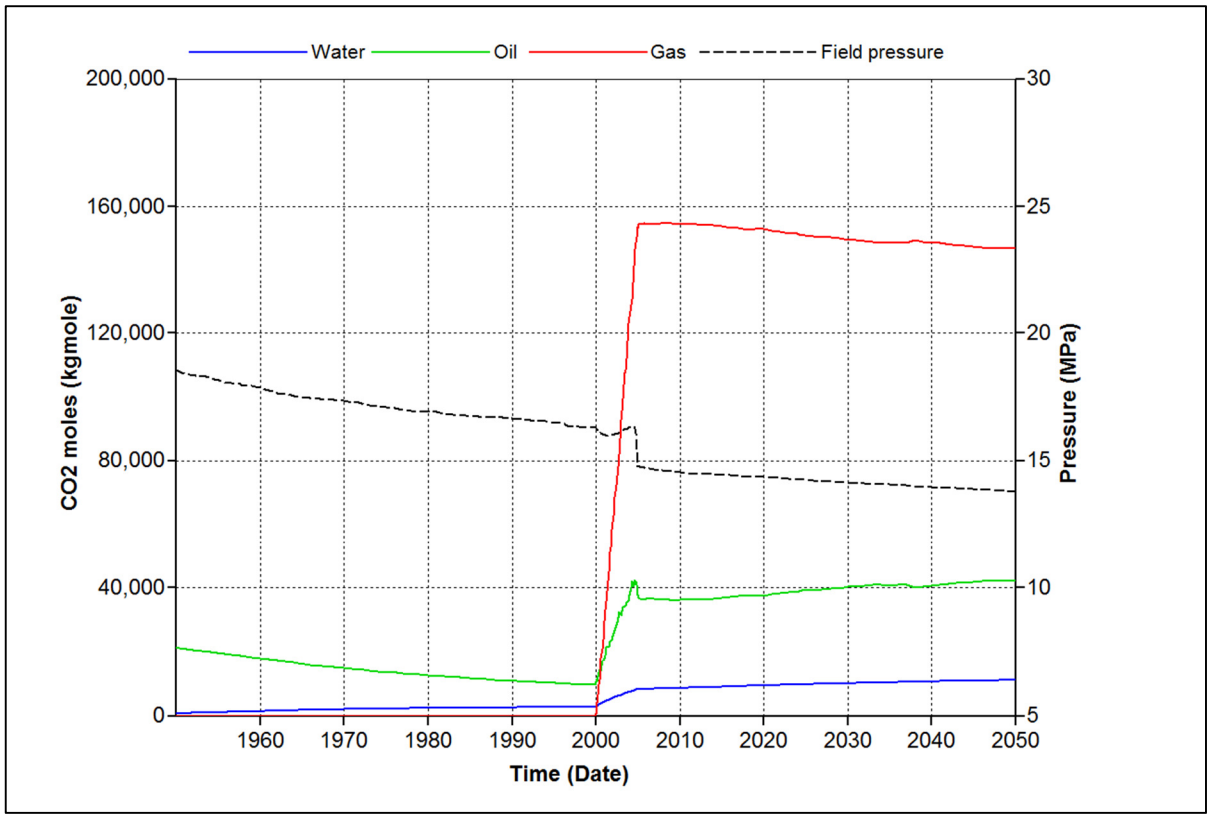

Figure 19. Simulation results for continuous gas injection (Case 1).

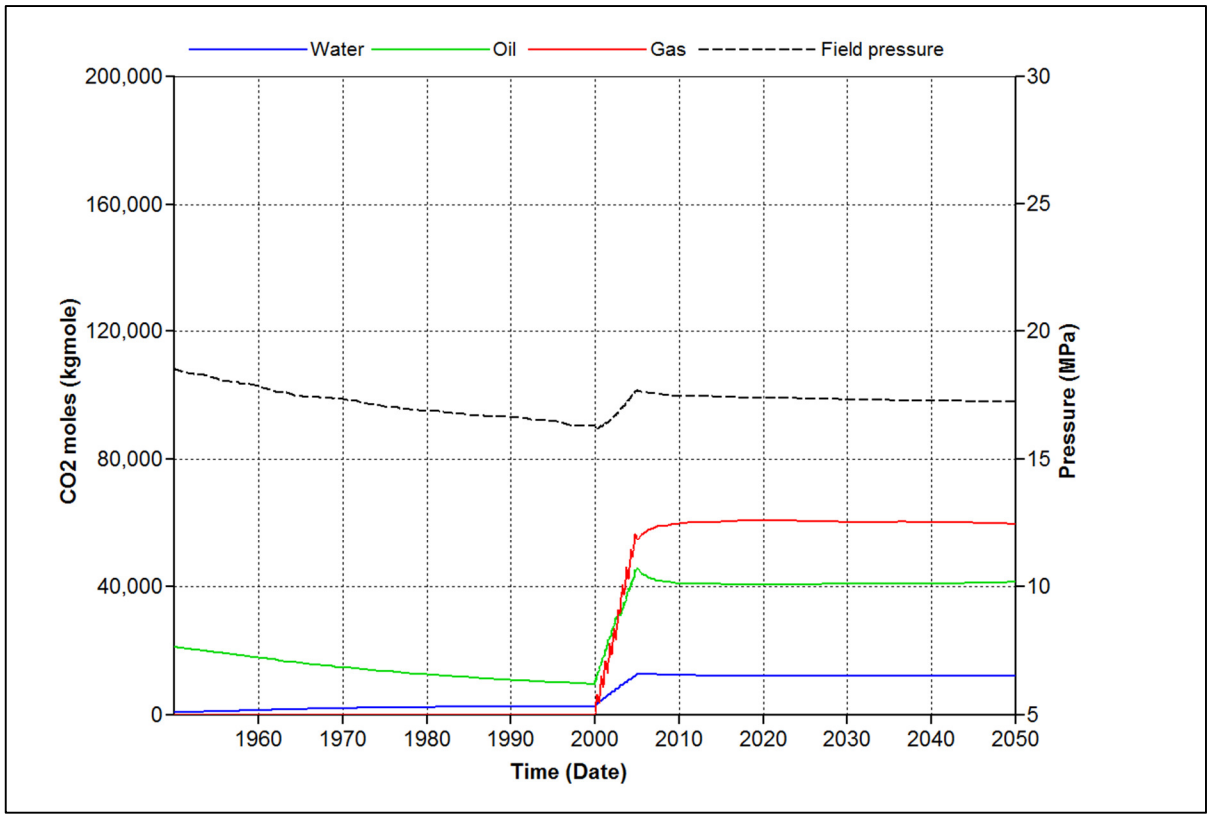

Figure 20. Simulation results for water-alternating gas injection (Case 2).

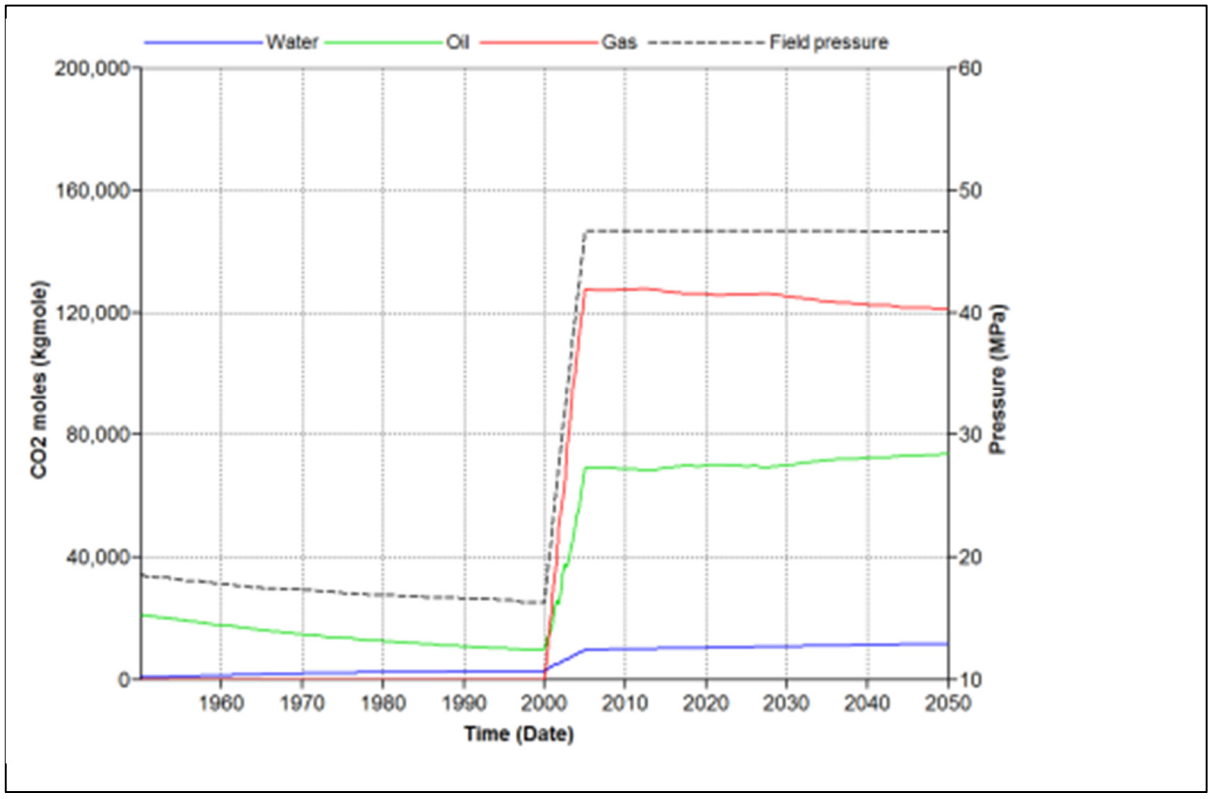

Figure 21. Simulation results for injection into a depleted oil field (Case 3).

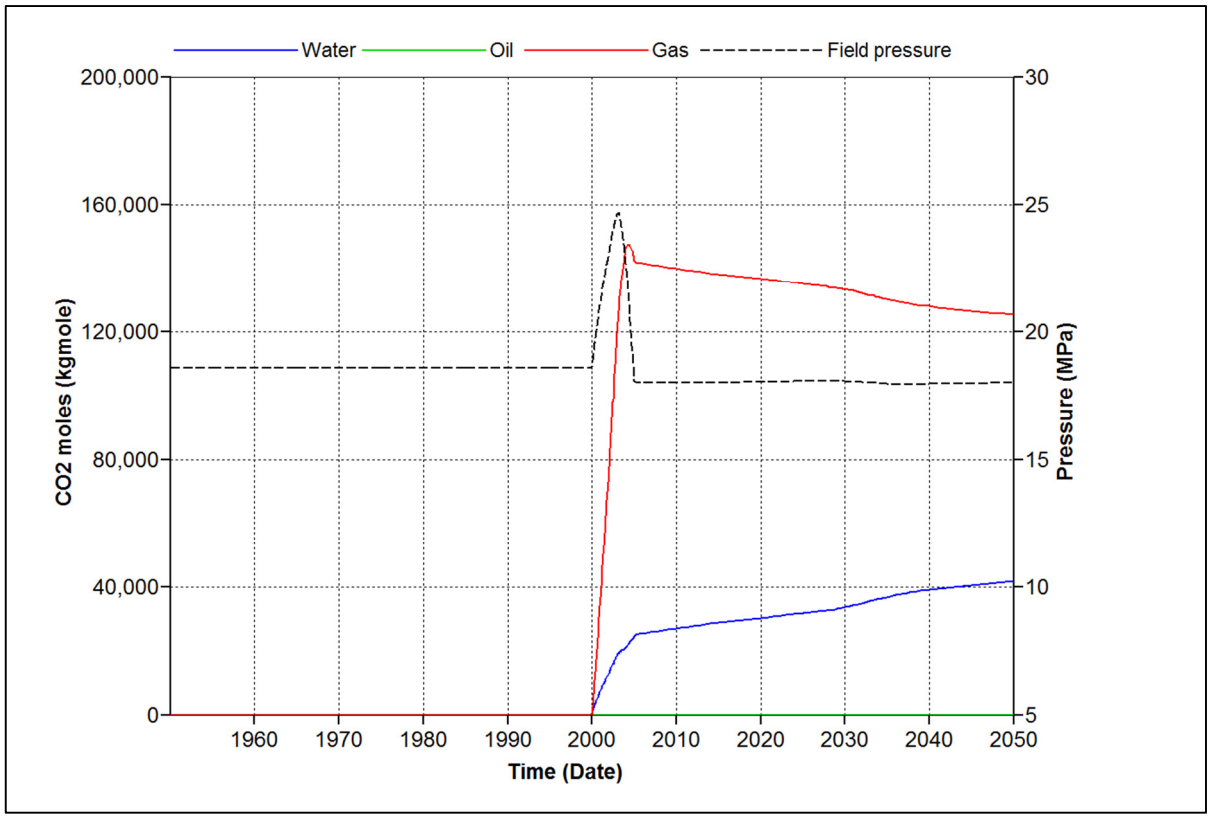

Figure 22. Simulation results for injection into an aquifer (Case 4).

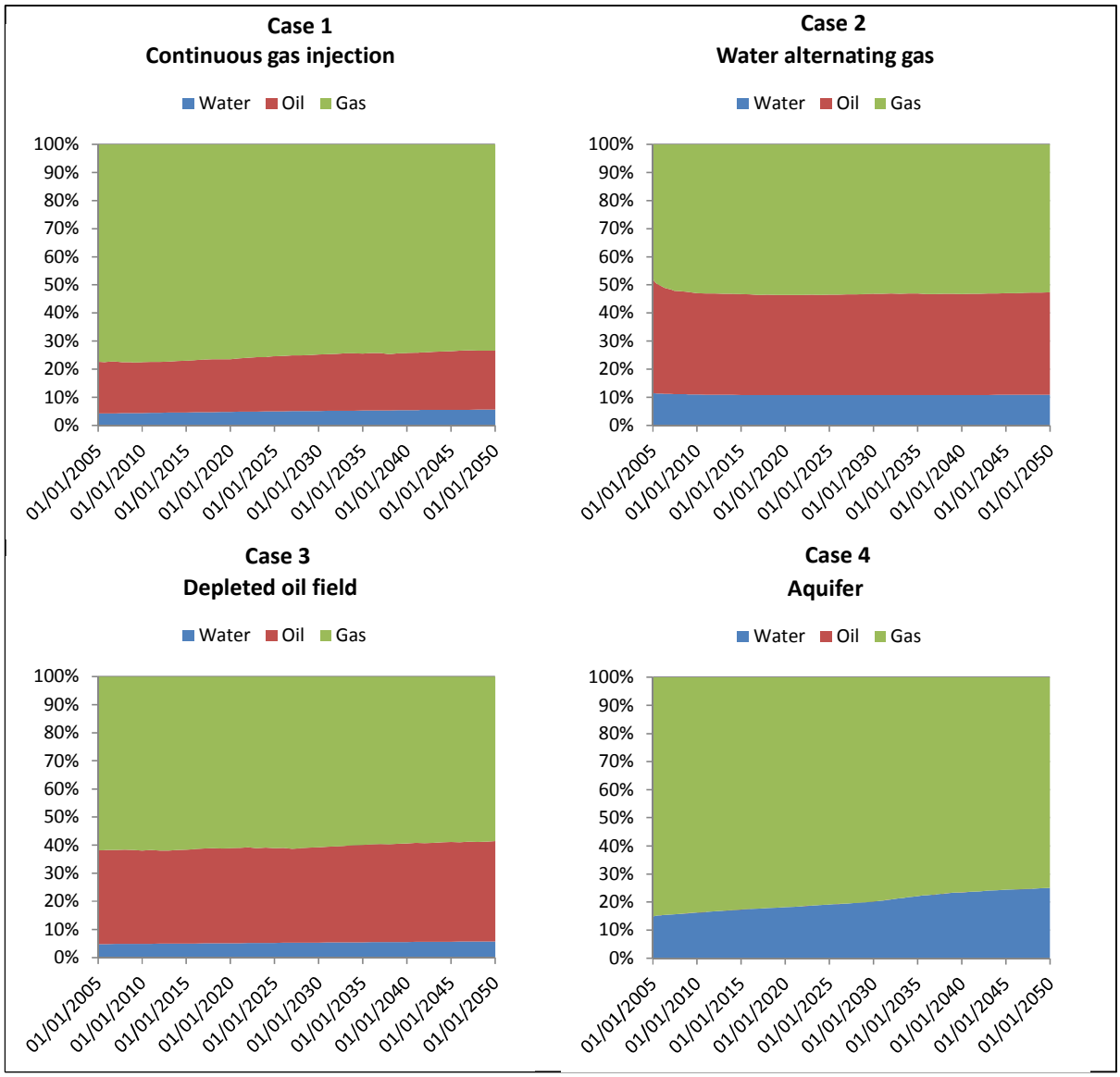

Figure 23. Comparison of the partitioning of CO_2 present in the water, oil and gas phases during a 45 year equilibration period following CO_2 injection for the cases modelled.

One proviso for these results is that the field pressure in these simulations falls below the MMP in all but the depleted oil field case. In the depleted oil field case there are no fluids produced during the injection period and hence the field pressure increases significantly.

5. Recommendations and Conclusions

The two geochemical methods described in section 3 of this report using empirical data show that the distribution of CO_2 in the reservoir, and hence the relative role of the trapping mechanisms, is closely matched where conditions permit both methods to work. Discrepancies do occur when there is not a free phase CO_2 present and hence the isotope approach does not work. Future work could develop the isotope technique further to account for this. However where these conditions are met the two methods accord very well (compare Fig 6 and Fig 10). The initial reservoir model simulation presented in section 4.1 of this report also closely matches the average CO_2 distribution and relative trapping contributions derived from the geochemical approaches. A slightly higher fraction of CO_2 dissolves in the oil and slightly lower fraction dissolves in the water when comparing the reservoir model to the average values of the geochemical data. However the modeled numbers are well within the ranges of the geochemical data giving extra confidence in both the methods using the empirical data and the reservoir model itself.

The simulation results indicate that for this approximative model of the PCCMP pilot, after injection ceases, the CO_2 has a greater affinity to dissolve in the oil rather than the water which matches the solubilites calculated in section 3 of this report at the Pembina field. Under the reservoir and fluid conditions in this system, when oil is present, more CO_2 dissolves in the oil than dissolves in the water. The CO_2 also dissolves more quickly in the oil than in the water.

Further work on ther reservoir modelling may be considered to quantify the amount of CO_2 present in the residual and mobile phases, and to consider the competition between optimisation of oil recovery and CO_2 storage. The former would require modifications to be made to the relative permeability curves to introduce hysteresis. Further enhancements could also be made to the model, introducing heterogeneity to the grid properties, validating the oil PVT properties and investigating the effect of grid resolution.

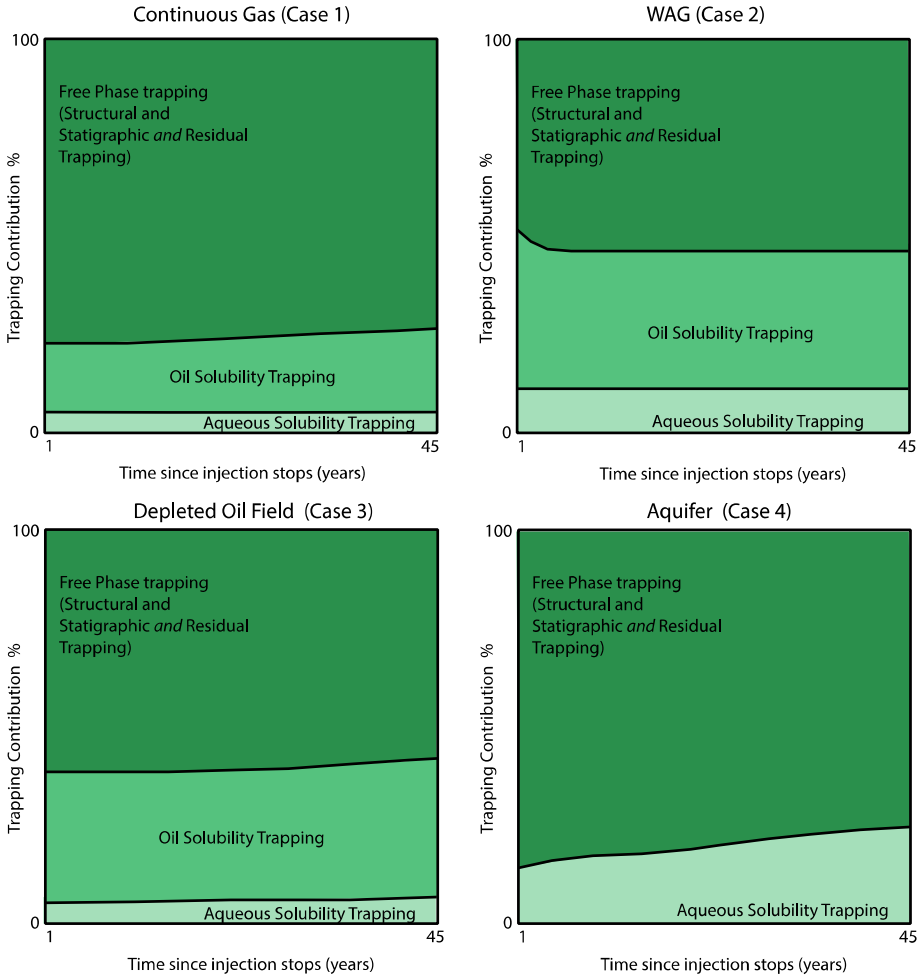

Figure 24. Trapping mechanisms for each case modelled.

Figure 24 shows a set of variations of figure 1 re-drawn for the cases modeled in this study but with a much shorter time-frame (45 years versus 10,000 years in figure 1). As such, mineral trapping is discarded as a process that will play a significant role in the short term. Where oil is present (Cases 1,2,3) more CO_2 will be dissolved in the reservoir fluids than for the case (4) where only CO_2 and water phases are present. The fraction of CO_2 that dissolves in the oil is greatest for WAG injection, despite the fact that only half the time of the injection period is spent injecting CO_2 and the other half of the time injecting water. Cases with oil present equilibrate more quickly than in the case with no oil present (aquifer). In the latter case there is still ongoing dissolution of CO_2 in the water taking place 50 years after injection started. The intial simulation model at the end of CO_2 injection (Case 0) shows significantly more CO_2 is dissolved in the fluids than in the cartoon of figure 1 (which shows ~10% solubility trapping after 2 years) whether you take the values from the model (32% solubility trapped) or from the average from the empirical data (approximately 25% solubility

trapped). The presence of oil in the subsurface is therefore beneficial to solubility trapping and hence enhanced security in this system.

Acknowledgements

CMG Ltd are thanked for the use of their WinProp, Builder, GEM and Results software and data in carrying out this work. University of Calgary are thanked for access to the geochemical monitoring and production data." to "The Applied Geochemistry group at the University of Calgary are thanked for collecting and help with interpreting the geochemical data.

References

Alberta Innovates 2005. Penn West Energy Trust Pembina Cardium 'A' Lease - CO2 Pilot Project Annual Report 2005. Retrieved Dec 2014 from http://eipa.alberta.ca/resources/co2/pembina.aspx

Alberta Innovates 2006. Penn West Energy Trust Pembina Cardium 'A' Lease - CO2 Pilot Project Annual Report 2006. Retrieved Dec 2014 from http://eipa.alberta.ca/resources/co2/pembina.aspx

Alberta Innovates 2007. Penn West Energy Trust Pembina Cardium 'A' Lease - CO2 Pilot Project Annual Report 2007. Retrieved Dec 2014 from http://eipa.alberta.ca/resources/co2/pembina.aspx

Arnott, R.W.C., 1992. The role of fluvial processes during the deposition of the (Cardium) Carrot Creek/Cyn-Pem conglomerates. Bulletin of Canadian Petroleum Geology, v.40, pp.356-362.

Bamberger, A., Sieder, G. & Maurer, G., 2000. High-pressure (vapor + liquid) equilibrium in binary mixtures of (carbon dioxide + water or acetic acid) at temperatures from 313 to 353 K. *Journal of Supercritical Fluids*, 17, pp.97–110.

Bell, J.S., and Bachu, S., 2003. In situ stress magnitude and orientation estimates for Cretaceous coal-bearing strata beneath the plains area of central and southern Alberta. Bulletin of Canadian Petroleum Geology, v.51, pp.1-28.

Bergman, K.M., and Walker, R.G., 1987. The importance of sea-level fluctuations in the formation of linear conglomerate bodies; Carrot Creek member of the Cardium Formation, Cretaceous Western Interior Seaway, Alberta, Canada. Journal of Sedimentary Petrology, v.57, pp.651-665.

Carroll, J.J. & Mather, A.E., 1992. The system carbon dioxide-water and the Krichevsky-Kasarnovsky equation. *Journal of Solution Chemistry*, 21(7), pp.607–621.

Chung, F.T.H., Jones, R.A. & Nguyen, H.T., 1988. Measurements and Correlations of the Physical Properties of CO_2/Heavy-Crude-Oil Mixtures. SPE Reservoir Engineering (August) 822.

Clarkson, C.R. & Pedersen, P.K., 2010. Tight Oil Production Analysis : Adaptation of Existing Rate-Transient Analysis Techniques. *Canadian Unconventional Resources & International Petroleum Conference Resources*, (1992), p.16.

CMG, 2014. Computer Modelling Group, *CO_2 EOR Modelling Using GEM - Course Notes*, 2014.

Crovetto, R., 1991. Evaluation of Solubility CO_2-H_2O from 273K to the Critical Point of Water. *J. Phys. Chem*, 20. 3.

Dashtgard, S.E., Buschkuehle, M.B.E., Fairgrieve, B., and Berhane, H., 2008. Geological characterization and potential for carbon dioxide (CO2) enhanced oil recovery in the Cardium Formation, central Pembina Field, Alberta. Bulletin of Canadian Petroleum Geology, v. 56, n.2, pp.147-164.

DeRuiter, R. A., Nash, L.J. & Singletary, M.S., 1994. Solubility and Displacement Behavior of a Viscous Crude With CO_2 and Hydrocarbon Gases. *SPE Reservoir Engineering*, 9(May), pp.101–106.

Diamond, L.W. & Akinfiev, N.N., 2003. Solubility of CO_2 in water from -1.5 to 100°C and from 0.1 to 100 MPa: Evaluation of literature data and thermodynamic modelling. *Fluid Phase Equilibria*, 208, pp.265–290.

Duan, Z., Møller, N. & Weare, J.H., 1992. An equation of state for the CH_4-CO_2-H_2O system: I. Pure systems from 0 to 1000°C and 0 to 8000 bar. *Geochimica et Cosmochimica Acta*, 56, pp.2605–2617.

Duan, Z. & Sun, R., 2003. An improved model calculating CO_2 solubility in pure water and aqueous NaCl solutions from 273 to 5333 K and from 0 to 2000 bar. *Chem Geol*, 193, pp.257–271.

Harvey, A.H.: "Semi-empirical Correlation for Henry's Constants over Large Temperature Ranges," AIChE J., Vol. 42, No. 5 (May 1996), pp. 1491-1494.

Hitchon, 2009. *Pembina Cardium CO_2 Monitoring Pilot: A CO_2-EOR Project, Alberta, Canada - Final Report*. Geoscience Publishing, 2009. ISBN 978-0-9680844-5-8.

IPCC, 2005. IPCC Special Report on Carbon Dioxide Capture and Storage. Prepared by Working Group III of the Intergovernmental Panel on Climate Change [Metz, B., Davidson, O., de Coninck, H.C., Loos, M., and Meyer, L.A., (eds.)]. Cambridge University Press, Cambridge, United Kingdom and New York, NY, USA, p.442.

Johnson, G., 2010. Stable Isotope Approaches to Monitoring and Verification of Injected CO_2 at the Pembina Cardium CO_2 Monitoring Pilot, Alberta, Canada. *PhD Thesis, University of Calgary*, (November).

Johnson, G., Mayer, B., Shevalier, M., Nightingale, M. & Hutcheon, I. 2011a. Tracing the movement of CO2 injected into mature oilfield using carbon isotope abundance ratios: The example of the Pembina Cardium CO2 Monitoring project. – International Journal of Greenhouse Gas Control, v.5, pp. 933-941. doi:10.1016/j.ijggc.2011.02003

Johnson, G., Mayer, B., Nightingale, M., Shevalier, M., & Hutcheon, I. 2011b. Using oxygen isotope ratios to quantitatively assess trapping mechanisms during CO_2 injection into geological reservoirs: The Pembina case study. *Chemical Geology*, 283(3-4), pp.185–193.

Justen, J.J., 1957. Canada's Pembina Field. Journal of Petroleum Technology, v.9,

n.9, pp.21-26.

Justen J.J., and Hoenmans, P.J.,1958. Pembina Pilot Flood Proving Successful. Journal of Petroleum Technology, v.10, n.6, pp.21-23.

Krause, F.F., and Nelson, D.A., 1984. Storm event sedimentations: Lithofacies association in the Cardium Formation, Pembina area, west-central Alberta, Canada. In Stott, D.F., and Glass, D.J., (eds), The Mesozoic of Middle North America. Canadian Society of Petroleum Geologists, Memoir 9, pp.485-511.

Krause, F.F., Collins, H.N., Nelson, D.A., Machemer, S.D., and French, P.R., 1987. Multiscale Anatomy of a Reservoir: Geological Characterization of Pembina-Cardium Pool, West-Central Alberta, Canada. *American Association of Petroleum Geologists Bulletin*, 71, pp.1233–1260.

Krause, F.F., Deutsch, K.B., Joiner, S.D., Barclay, J.E., Hall, R.L., and Hills, L.V., 1994. Cretaceous Cardium Formation of the Western Canada Sedimentary Basin. In Mossop, G.D., and Shetsen, I., (eds), Geological Atlas of the Western Canada Sedimentary Basin. Canadian Society of Petroleum Geologists. pp.375-385.

Lécuyer, C., Gardien, V., Rigaudier, T., Fourel, F., Martineau, F., and Cros, A., 2009. Oxygen isotope fractionation and equilibration kinetics between CO_2 and H_2O as a function of salinity of aqueous solutions. *Chemical Geology*, 264(1-4), pp.122–126. Available at: http://dx.doi.org/10.1016/j.chemgeo.2009.02.017.

Leggitt, S.M., Walker, R.G. & Eyles, C.H., 1990. Control of reservoir geometry and stratigraphic trapping by erosion surface E5 in the Pembina-Carrot Creek area, Upper Cretaceous Cardium Formation, Alberta, Canada. *American Association of Petroleum Geologists Bulletin*, 74, pp.1165–1182.

Miller, J. & Jones, R., 1981. A Laboratory Study to Determine Physical Characteristics of Heavy Oil After CO_2 Saturation. *Proceedings of SPE/DOE Enhanced Oil Recovery Symposium*. Available at: http://dx.doi.org/10.2118/9789-MS.

Owen, E.W., 1975. Trek of the oil finders: a history of exploration for petroleum. AAPG Memoir 6, 1647 p.

Penn West Energy Trust, 2005. Pembina Cardium 'A' Lease - CO_2 Pilot Project: Annual Report - 2005.

Penn West Energy Trust, 2006. Pembina Cardium 'A' Lease - CO_2 Pilot Project: Annual Report - 2006.

Penn West Energy Trust, 2007. Pembina Cardium 'A' Lease - CO_2 Pilot Project: Annual Report - 2007.

Pitzer, K.S., 1973. Thermodytriarnics of Electrolytes. I. Theoretical Basis and General Equations. *The Journal of Physical Chemistry*, 77(6), pp.268–277. Available at: http://pubs.acs.org/doi/abs/10.1021/j100621a026.

Plint, A.G., Walker, R.G., and Bergman, K.M., 1986. Cardium Formation 6. Stratigraphic framework of the Cardium in subsurface. Bulletin of Canadian Petroleum Geology, v.34, pp. 213-225.

Plint, A.G., Walker, R.G., and Duke, W.L., 1988. An outcrop to subsurface correlation of the Cardium Formation in Alberta. In James, D.P., and Leckie, D.A., (eds), Sequences, Stratigraphy, Sedimentology: Surface and Subsurface. Canadian Society of Petroleum Geologists, Memoir 15, pp.167-184.

Shevalier, M., Nightingale, M., Johnson, G., Mayer, B., Perkins, E., and Hutcheon, I., 2009. Monitoring the reservoir geochemistry of the Pembina Cardium CO2 monitoring project, Drayton Valley, Alberta. Energy Procedia, v.1, n.1, pp.2095-2102. doi:10.1016/j.egypro.2009.01.273.

Shyu, G.-S., Hanif, N.S.M., Hall, K.R., & Eubank, P.T., 1997. Carbon dioxide-water phase equilibria results from the Wong-Sandler combining rules. *Fluid Phase Equilibria*, 130, pp.73–85.

Simon, R. & Graue, D. 1965. Generalized Correlations for Predicting Solubility, Swelling & Viscosity Behavior of CO_2-Crude Oil Systems. *J. Pet. Techn.* v.17, n.1, *102-106*.

Spycher, N., Pruess, K. & Ennis-King, J., 2003. CO_2-H_2O mixtures in the geological sequestration of CO_2. I. Assessment and calculation of mutual solubilities from 12 to 100C and up to 600 bar. *Geochimica et Cosmochimica Acta*, 67(16), pp.3015–3031.

Stalkup, F.I., 1978. Carbon Dioxide Miscible Flooding: Past, Present, And Outlook for the Future. *Journal of Petroleum Technology*, 30. n.8, pp.1102-1112

Stevens, L.C., Bird, S.F., and Justen, J.J., 1959. The Pembina Oil Field, Alberta, Canada – An example of a Low Permeability Reservoir. Proceedings of the 5th World Petroleum Congress, Section II, 173-185, New York.

Welker, J.R. & Dunlop, D.D., 1963. The Physical Properties of Carbonated Oils. *J. Pet.Techn.* v.15. pp.873–875.

Worden, R.H. & Smith, L.K., 2004. Geological sequestration of CO_2 in the subsurface: lessons from CO_2 injection enhanced oil recovery projects in oilfields. *Geological Society, London, Special Publications*, 233, pp.211–224.